Published in final edited form as:
*Virology*. 2012 July 20; 429(1): 74–90. doi:10.1016/j.virol.2012.04.005.

# Wildtype coxsackievirus infection dramatically alters the abundance, heterogeneity, and immunostimulatory capacity of conventional dendritic cells in vivo

**Christopher C. Kemball**[a,*], **Claudia T. Flynn**[a], **Martin P. Hosking**[a], **Jason Botten**[b], and **J. Lindsay Whitton**[a]

[a]Department of Immunology and Microbial Science., SP30-2110, The Scripps Research Institute, 10550 N. Torrey Pines Rd., La Jolla, CA 92037, USA

[b]Department of Medicine, University of Vermont College of Medicine, Burlington, VT 05405, USA

## Abstract

*In vitro* studies have shown that enteroviruses employ strategies that may impair the ability of DCs to trigger T cell immunity, but it is unclear how these viruses affect DCs *in vivo*. Here, we evaluate the effects of wild-type (wt) coxsackievirus B3 on DCs *in vitro* and in a murine model *in vivo*. Although CVB3 does not productively infect the vast majority of DCs, virus infection profoundly reduces splenic conventional DCs numbers and diminishes their capacity to prime naïve $CD8^+$ T cells *in vitro*. In contrast to recombinant CVB3, highly pathogenic wt virus infection significantly diminishes the host's capacity to mount T cell responses, which is temporally associated with the loss of $CD8\alpha^+$ DCs. Our findings demonstrate that enterovirus infection substantially alters the number, heterogeneity, and stimulatory capacity of DCs *in vivo*, and these dramatic immunomodulatory effects may weaken the host's capacity to mount antiviral T cell responses.

### Keywords

coxsackievirus; lymphocytic choriomeningitis virus; dendritic cell; T cell; mouse; spleen; infection; immunity

## Introduction

Dendritic cells (DCs) are specialized antigen presenting cells that link the immediate innate immune response to viral infection with the subsequent generation of an adaptive immune response (Lee and Iwasaki, 2007). DCs comprise 2 major groups, plasmacytoid DCs (pDC) and conventional DCs (cDC). pDCs play an important role in shaping the innate and adaptive antiviral immune responses by their ability to secrete large amounts of type I interferon (IFN) in response to viral nucleic acid recognition (Gilliet *et al.*, 2008; Swiecki and Colonna, 2010b). Although pDCs are capable of antigen presentation (Villadangos and



*Corresponding author, CC Kemball, Dept. of Immunology and Microbial Science., SP30-2110, The Scripps Research Institute, 10550 N. Torrey Pines Rd., La Jolla, CA 92037, USA. cckemball@gmail.com Tel: 1-858-784-7094 Fax: 1-858-784-7377.

Young, 2008), it is the cDCs that play a major role in priming virus-specific T cell responses (Heath and Carbone, 2009; Lopez-Bravo and Ardavin, 2008). cDCs in the spleen can be divided into 3 major subsets: $CD8\alpha^+$ DCs, $CD4^+$ DCs, and $CD8^-CD4^-$ "double negative" DCs. These subsets also are found in peripheral lymph nodes, along with other subsets of migratory conventional DCs (Heath and Carbone, 2009; Lopez-Bravo and Ardavin, 2008). In addition, the inflammatory environment generated by virus infection can trigger the differentiation of monocyte-derived DCs that contribute to antiviral immunity and stimulate virus-specific T cell responses (Dominguez and Ardavin, 2010; Leon and Ardavin, 2008). Studies have shown that cDC subsets exert distinct functions in activating antiviral T cell responses. $CD8\alpha^+$ DCs are particularly efficient at capturing apoptotic cells and priming virus-specific $CD8^+$ T cell responses. In contrast, $CD8\alpha^-$ DCs are specialized for processing and presentation of antigens on MHC class II and preferentially trigger $CD4^+$ T cell responses (Lopez-Bravo and Ardavin, 2008; Segura and Villadangos, 2009; Shortman and Heath, 2010; Villadangos and Schnorrer, 2007). The functional specialization of $CD8\alpha^+$ and $CD8\alpha^-$ subsets may be related to differences in their expression of viral RNA sensors and/or machinery involved in antigen processing and presentation (Dudziak *et al.*, 2007; Luber *et al.*, 2010).

Type B Coxsackieviruses (CVB) are important human pathogens that belong to the Picornavirus family and human enterovirus B genus. A considerable proportion of CVB infections trigger severe acute and chronic diseases and cause morbidity and mortality, particularly in infants, young children, and immunocompromised individuals (Modlin and Rotbart, 1997; Romero, 2008; Whitton, 2002). CVB are the most common cause of infectious myocarditis, a serious disease that can lead to dilated cardiomyopathy and cardiac failure (O'Connell, 1987; Sole and Liu, 1993; Tam, 2006). These viruses also can induce other diseases, including pancreatitis, aseptic meningitis, and encephalitis (Daley *et al.*, 1998; Feuer *et al.*, 2005; Huber and Ramsingh, 2004; Mena *et al.*, 2000; Rhoades *et al.*, 2011; Tracy and Chapman, 2010). Control of CVB infection depends on both humoral and cell mediated-immunity (Kemball *et al.*, 2010a; Kemball *et al.*, 2010b). $CD8^+$ T cell responses directed at native epitopes in the CVB polyprotein are remarkably weak (Jakel *et al.*, 2009; Varela-Calvino *et al.*, 2004; Voigt *et al.*, 2010; Weinzierl *et al.*, 2008a) and, in order to enhance our ability to detect virus-specific T cells, our laboratory generated recombinant CVB3 (rCVB3) that encode well characterized $CD8^+$ and/or $CD4^+$ T cell epitopes from lymphocytic choriomeningitis virus (LCMV). Despite their ability to replicate to high titers *in vivo*, wild-type (wt) CVB3 and rCVB3 induce minimal T cell activation and weak endogenous virus-specific T cell responses (Crocker *et al.*, 2007; Kemball *et al.*, 2008; Slifka *et al.*, 2001). Using epitope-specific $CD8^+$ transgenic T cells as sensors to evaluate *in vivo* antigen presentation by rCVB3, we demonstrated that this virus almost completely evades presentation through the MHC class I pathway (Kemball *et al.*, 2009). This strategy is extremely effective, as naïve virus-specific $CD8^+$ transgenic T cells fail to expand in rCVB3-infected mice. Memory $CD8^+$ T cells, however, can respond to a lower level of antigen presentation than their naïve counterparts (Slifka and Whitton, 2001), and we found that epitope-specific memory $CD8^+$ T cells were activated by rCVB3 infection *in vivo* (Kemball *et al.*, 2008). Therefore, we have suggested that the quantity of MHC class I/viral peptide complex that is expressed on a CVB3-infected cell is too low to trigger strong responses by naïve $CD8^+$ T cells, but is sufficient to activate memory $CD8^+$ T cells.

Activation of naïve $CD8^+$ T cells is profoundly dependent upon antigen presentation by cDCs. However, the effects of coxsackievirus infection on dendritic cell populations *in vivo* are not well understood. *In vitro* studies have shown that other enteroviruses can infect DCs and employ tactics that may impair the ability of DCs to prime robust T cell responses. Poliovirus, a close relative of CVB, can inhibit protein synthesis in DCs and dampens MHC class I antigen presentation (Choe *et al.*, 2005; Deitz *et al.*, 2000; Wahid *et al.*, 2005); the

virus also inhibits proinflammatory cytokine secretion and the expression of antiviral cytokine receptors (Dodd *et al.*, 2001; Neznanov *et al.*, 2001). Furthermore, echovirus infection limits the ability of DCs to up-regulate costimulatory molecules and to produce cytokines following TLR stimulation (Kramer *et al.*, 2007). However, it is not known whether picornaviruses exert similar effects on DCs *in vivo*. A recent study reported that positive and negative strand CVB3 RNA was present in DCs following infection *in vitro* and *in vivo* but, in both cases, viral replication was incomplete and the infection was non-productive (Weinzierl *et al.*, 2008b). It is unclear what frequency of DCs is infected by CVB3 *in vivo*, and whether the virus can modulate presentation of viral epitopes at the surface of these professional antigen presenting cells. Furthermore, infection of the host may indirectly affect DCs, quantitatively and/or qualitatively, potentially limiting their ability to trigger T cell responses. We have previously shown that rCVB3 did not globally suppress the host's capacity to mount $CD8^+$ T cell responses (Kemball *et al.*, 2009); however, rCVB3 are attenuated *in vivo*, and we considered it vital to determine if highly-pathogenic wild-type (wt) virus profoundly affects one or more DC subsets *in vivo*, and whether such changes are associated with a reduced ability of the host to trigger strong antiviral T cell responses.

In this study, we have used the murine model of CVB3 infection to evaluate the effects of the wt virus on dendritic cells *in vivo*. We report that, for the vast majority of DCs *in vitro* and *in vivo*, we observe neither productive infection nor viral protein synthesis. Nevertheless, wtCVB3 infection rapidly induces phenotypic changes in conventional DCs *in vivo*, and also dramatically reduces their abundance. *In vitro* analyses show that splenocytes taken from wtCVB3-infected mice have a diminished capacity to stimulate naïve T cells; however, on a per-cell basis, DCs from wtCVB3-infected mice remain capable of triggering $CD8^+$ T cell division. In contrast to rCVB3, wt virus infection significantly diminished the host's capacity to mount T cell responses, which was temporally associated with the loss of $CD8\alpha^+$ DCs. To our knowledge, our study is the first to precisely enumerate cDCs during picornavirus infection, and to show that their abundance is substantially altered *in vivo*.

## Results

### CVB3 infection substantially alters conventional and plasmacytoid dendritic cell populations in vivo

We first examined whether CVB infection had any quantitative or qualitative effect on conventional and plasmacytoid DCs *in vivo*. Mice were inoculated with $10^3$ PFU of wild-type CVB3 (wtCVB3). Virus replicated rapidly and reached very high titers in the pancreas on day 2–4 p.i. ($>10^{10}$ PFU/g), then declined by day 6 (Figure 1A). In contrast to many acute virus infections, which induce mild or moderate splenomegaly together with strong virus-specific $CD8^+$ T cell responses, acute infection with wtCVB3 was associated with a gradual and substantial reduction in the total number of splenocytes, which declined ~4-fold by day 8 compared to uninfected mice (Figure 1B). Because primary virus-specific T cell responses are usually initiated within a few days of infection, we analyzed conventional and plasmacytoid DCs numbers on days 2, 4, 6, and 8 p.i. cDCs were classified as $CD11c^{hi}$ and negative for expression of lineage markers for T cells, B cells, and NK cells ($CD3^-CD19^-CD49b^-$). pDCs were defined by being CD11c intermediate ($CD11c^{int}$), lineage negative, and expressing high levels of bone marrow stromal cell antigen 2 (BST-2, also known as mPDCA-1). cDCs were readily detected in uninfected mice, but declined in CVB3-infected mice after day 2, and very few of these cells remained by day 8 (Figure 1C & E). pDCs also were detected in uninfected mice, and their total number increased ~8-fold in virus-infected mice by day 6 and then declined by day 8 (Figure 1D); their frequency, too, increased markedly between 4 and 6 days p.i. (Figure 1F). Thus, CVB3 infection substantially alters the frequency and number of both conventional and plasmacytoid DCs.

### CVB3 infection dramatically reduces the subset of conventional dendritic cells that is thought to be the most potent inducer of antiviral CD8$^+$ T cell responses

Conventional DCs, and in particular their CD8α$^+$ subset, are known to be very efficient at priming virus-specific CD8$^+$ T cell responses (Shortman and Heath, 2010). To evaluate the effects of wtCVB3 infection on these cells, splenocytes were harvested from infected mice on days 2, 4, 6, and 8, stained with antibodies to discriminate among the 3 major subsets of conventional DCs, and analyzed by flow cytometry. As expected, and in order of decreasing frequency, CD4$^+$, double negative, and CD8α$^+$ subsets were detected among CD11c$^{hi}$ DCs in uninfected spleens (Figure 2A, top left panel). The frequency of CD8α$^+$ DCs increased slightly on day 2, and then declined sharply thereafter; very few CD8α$^+$ DCs remained in the spleen from day 4 onward (Figure 2A, C & D). The frequency of CD4$^+$ DCs also declined dramatically following CVB3 infection (Figure 2A, & C) and, by 8 days p.i., the number of these cells had decreased almost 40-fold compared to uninfected animals (Figure 2D). Double negative DCs were proportionately less affected by infection, and became the dominant subset by day 4 (as a percentage of all DCs, Figure 2A & C). However, the absolute number of all three cDC subsets declined over the course of infection (Figure 2D). We next focused on the CD205$^+$ subset of CD8α$^+$ cDCs. These cells are potent inducers of antiviral CD8$^+$ T cell responses *in vivo* and are thought to be specialized for the processing and presentation of exogenous antigens on MHC class I (cross-presentation) (Dudziak *et al.*, 2007; Lopez-Bravo and Ardavin, 2008; Villadangos and Schnorrer, 2007). Previous findings from our laboratory have suggested that cross-priming is inefficient during CVB3 infection (Kemball *et al.*, 2009; Kemball *et al.*, 2008), and led us to question whether the virus modifies the CD8α$^+$CD205$^+$ cDC subset *in vivo*. The frequency and number of CD8α$^+$CD205$^+$ cDCs shared similar kinetics with the total CD8α$^+$ cDC population, and virus infection led to a dramatic reduction in number of CD8α$^+$CD205$^+$ cDCs by day 4 (Figure 2B & E). Taken together, these data show that CVB3 infection substantially modifies the relative proportions of cDC subsets, and is associated with a profound reduction in the number of all cDC subsets, including the cells that are optimally suited to prime virus-specific CD8$^+$ T cell responses.

To assess whether this loss of DCs occurs in other secondary lymphoid organs, we evaluated the effects of wtCVB3 infection on DC populations in the pancreatic lymph nodes (pLNs). The frequency of CD8α$^+$ DCs in the pLNs declined sharply after day 2 p.i. in a similar manner to CD8α$^+$ DCs in the spleen (Figure 2C & Figure 3A). The total number of CD11c$^{hi}$ DCs, and the number of all three DC subsets also declined after infection; few CD8α$^+$ DCs remained in the pLNs from day 4 onward (Figure 3B–D). In addition, very few CD11c$^{hi}$ cDCs were present in virus-infected pancreas; although other lymphocytes (T cells, macrophages, neutrophils) were readily detected in this organ following infection, DCs were present at a very low level and their numbers did not increase with infection (data not shown). Overall, CVB3 infection leads to a similar reduction in cDCs in the spleen and pLNs.

### CVB3 infection does not globally inhibit the up-regulation of MHC and costimulatory molecules on conventional dendritic cells in vivo

Besides reducing the number of DCs available for presenting viral antigen and/or priming virus-specific T cells *in vivo*, CVB3 also could avoid activating naïve T cells by limiting the expression of MHC and costimulatory molecules on the remaining DCs. To assess this, mice were infected with wtCVB3, and the cell surface phenotypes of the three major subsets of cDCs were analyzed. The levels of MHC class I, class II, and CD80 increased ~2-fold on CD8α$^+$ DCs by day 2, while CD40 and CD86 were more strongly up-regulated (~3-fold and ~5-fold, respectively) (Figure 4, top row). Because of the profound reduction in the frequency and number of CD8α$^+$ DCs by day 4 (Figure 2), we were unable to track the

phenotype of this subset at later time points. The $CD4^+$ and double negative subsets of DCs also expressed elevated levels of MHC class I, class II, CD40, and CD80 by day 2, although the increase was quite modest (≤ 2-fold); the level of these molecules was maintained, or decreased slightly, between 2 and 6 days post infection (Figure 4, middle and bottom rows). In contrast, CD86 expression was substantially up-regulated on $CD4^+$ and double negative subsets on day 2 (~4-fold), and then declined by day 4 (middle and bottom rows). Overall, the 3 major subsets of cDCs in the spleen displayed an activated phenotype within 48 hrs of CVB3 infection, and strongly up-regulated the costimulatory molecule CD86. A recent study examined changes in $CD11c^+$ DC phenotype *in vivo* at 36 hrs post CVB3 infection, but failed to detect a substantial change in MHC class I and II expression at this time point (Rahnefeld *et al.*, 2011). In contrast, our detailed analysis of cDC subsets revealed that $CD8\alpha^+$ DCs up-regulate these MHC molecules by 48 hrs p.i. (Figure 3, top row). These data suggest that the virus does not prevent the activation of splenic cDCs; on the contrary, $CD8\alpha^+$ DCs display a mature phenotype and appear poised to prime CVB3-specific $CD8^+$ T cells within the first 2 days of infection.

## Infection with a recombinant virus expressing DsRed suggests that very few DCs are infected in vivo

One obvious explanation for the dramatic reduction in DC numbers was that the virus directly infects DCs. In support of this idea, a recent study found that CVB3 could infect DCs, and both positive and negative strand viral RNA was detected in DCs *in vitro* and *in vivo* (Weinzierl *et al.*, 2008b). However, the proportion of DCs that were infected was not reported, viral replication was incomplete and non-productive, and viral protein synthesis within the cells was not assessed. Thus, we have assessed these issues, *in vivo* and *in vitro*. To investigate whether CVB3 proteins were expressed in cDCs *in vivo*, we used a rCVB3 that expresses DsRed (DsRed-CVB3, ref Tabor-Godwin *et al.*, 2010). Mice were infected with this virus and, to confirm infection and DsRed expression, we evaluated virus titers at days 1 & 2 post infection (p.i.), and used confocal microscopy to analyze tissue sections; the studies focused on the pancreas, a primary target organ of CVB3 *in vivo*. Viral titers were high (~$10^9$ pfu/g) at both time points, and DsRed expression was readily detected in many pancreatic acinar cells at 2 days p.i. (Figure 5A), indicative of successful infection and marker protein expression *in vivo*. Next we evaluated DsRed expression in DCs from the spleen and pancreatic lymph nodes (pLNs) at days 1 and 2 p.i., using flow cytometry. Several thousand DCs were analyzed in both tissues (~$3–7\times10^3$ cells per sample), but the frequency of $DsRed^+$ DCs was very low and similar to the background level seen in uninfected mice (Figure 5B). The differences in the percentage of $DsRed^+$ DCs between uninfected and infected mice were not statistically significant by a t-test comparing uninfected versus day 1 (spleen p=0.6266, pLNs p=0.0939) and uninfected versus day 2 (spleen p= 0.7664, pLNs p=0.2746). Flow cytometric analysis of DsRed expression in $CD8\alpha^+$, $CD4^+$, and double negative subsets of conventional DCs in the spleen yielded similar results (data not shown). Although very slightly more $DsRed^+$ DCs were identified in infected mice, the intensity of the fluorescent signal was low, and comparable to the negative control fluorescence intensity observed in DCs from uninfected mice (Figure 5B). We conclude that very few, if any, DCs express this CVB3 protein following infection *in vivo*.

## CVB3 and dendritic cells in vitro: no productive infection, protein synthesis, or down-regulation of MHC expression

The above data suggest that DCs are not a primary target for CVB3 infection *in vivo*, but we considered it important to determine if DCs might be susceptible to *in vitro* infection. An *in vitro* approach allowed us to generate large numbers of DCs, expose them to CVB3 synchronously at high moi, and characterize the progress of infection at defined time points

thereafter. Two different populations of DCs were analyzed: immature C57BL/6 bone marrow monocyte-derived DCs (cultured with GM-CSF); and DC2.4 cells, an immortalized cell line generated from C57BL/6 monocyte-derived DCs (Shen *et al.*, 1997). DCs were exposed to wtCVB3, or to a recombinant CVB3 expressing eGFP (eGFP-CVB3), at a high multiplicity of infection (MOI=10), or were mock infected; 22–23 hrs later the cells were stained for intracellular expression of the viral capsid protein VP1 and analyzed by flow cytometry to detect VP1 ± eGFP. HeLa cells were infected as a positive control. As expected, viral proteins were readily detected in HeLa cells (6 hrs post infection); for both viruses, ~90% of HeLa cells were $GFP^+$ and/or $VP1^+$ (Figure 6A, top row). In contrast, we did not detect a significant number of DCs that were $VP1^+$ or $GFP^+$; 96.5–99.5% of DCs were negative for CVB protein expression (Figure 6A, middle & bottom rows). Furthermore, no increase in virus titer was detected in infected DC2.4 or BMDC cultures, nor did we observe virus-induced cytopathic effect (not shown). Thus, there is little evidence that the majority of DCs can be productively infected by CVB3; indeed, the absence of viral protein synthesis in DCs suggests that even non-productive infection is very unusual. Moreover, no substantial changes to MHC class I, or II was observed on BMDCs 18–24 hrs after exposure to CVB3 *in vitro* (Figure 6B); this was true, too, of CD86 (not shown). Taken together, the data in Figure 5 and Figure 6 suggest that the great majority of DCs are resistant to CVB3 infection. Therefore, the dramatic reduction in DC numbers that follows CVB3 infection *in vivo* does not appear to result from direct infection-mediated cell death of DCs (Figure 1 & Figure 2).

## The loss of conventional dendritic cells in CVB3-infected mice is associated with weaker T cell responses to a secondary virus infection

We have previously shown that infection of mice with rCVB3 does not weaken their ability to mount T cell responses against a subsequent infection with LCMV. Rather, mice that receive rCVB3 three days before LCMV mount larger LCMV-specific T cell responses than mice infected with LCMV alone (Kemball *et al.*, 2009). However, rCVB3 are attenuated *in vivo*, and in light of the profound changes in $CD8\alpha^+$ DC numbers that accompany wtCVB3 infection, we considered it important to determine if the highly pathogenic wt virus would reduce the ability of the host to mount a subsequent antiviral T cell response to LCMV. Studies have shown that priming of LCMV-specific $CD8^+$ T cells requires DCs, and that $CD8\alpha^+$ cDCs are the predominant subset that initiates this response (Belz *et al.*, 2005; Probst and van den, 2005). We reasoned that the loss of $CD8\alpha^+CD205^+$ DCs in the spleen of wtCVB3-infected mice between 2 and 4 days p.i. (Figure 2B & E) might be associated with diminished T cell responses to LCMV that was inoculated 3 or 4 days post-wtCVB3. Therefore, groups of mice were infected with wtCVB3, and then co-infected with LCMV 3 or 4 days later. The frequencies of total $CD8^+$ and $CD4^+$ T cells, and LCMV-specific $CD8^+$ and $CD4^+$ T cell responses, were analyzed in the spleen 7 days after LCMV infection. Our analyses of co-infected mice (presented in Figure 7–Figure 12) were carried out in animals that exhibited clear indications of a robust CVB3 infection, by meeting three criteria: the presence of infectious virus in the feces (determined by plaque assay, 2 days after CVB3 infection); the presence of infectious virus in the pancreas (assayed at the time point of animal sacrifice and T cell analysis); and the presence of calcium deposits in the peritoneal cavity, a classic phenotypic signature of CVB3 infection and pancreatic disease (Mena *et al.*, 2000). The total number of mononuclear cells in the spleen (Figure 7A) and the frequency of splenic $CD8^+$ T cells (Figure 7B) were significantly reduced (~2–3 fold) in mice that had received wtCVB3 3 or 4 days before LCMV, as compared to mice that received LCMV infection alone. In contrast, the frequency of $CD4^+$ T cells was not significantly altered by CVB3 co-infection (Figure 7C). In mice that had received wtCVB3 3 or 4 days before LCMV, the total numbers of $GP_{33}$- and $NP_{396}$-specific $CD8^+$ T cells were significantly lower than in mice infected only with LCMV; when 4 days elapsed between wtCVB and

LCMV infections, the LCMV-specific T cell responses were 10- to 14-fold lower (Figure 7D). Mice that had received wtCVB3 4 days before LCMV did not have a lower frequency of total $CD4^+$ T cells (Figure 7C), but the overall reduction in splenocyte numbers (Figure 7A), combined with a reduced frequency of $GP_{61}$-specific cells among total $CD4^+$ T cells (not shown), led to a strong and significant reduction in the total number of $GP_{61}$-specific $CD4^+$ T cells, to an extent very similar to that observed for $CD8^+$ T cells (~14-fold; Figure 7E).

## The effect of wtCVB3 on T cell responses to LCMV appears early, but its impact is time-dependent

The data in Figure 7 show that wtCVB3 infection limits the T cell response to LCMV administered 4 days later, a time point at which $CD8\alpha^+CD205^+$ DCs in the spleen have reached their numerical nadir (Figure 2). In contrast to their status at day 4 following wtCVB3 infection, $CD8\alpha^+CD205^+$ DCs are abundant in the spleen at day 2 p.i., and display and activated phenotype (Figure 2B & E, Figure 4). Therefore, we considered the possibility that these abundant and highly-activated $CD8\alpha^+$ DCs might enhance, rather than limit, T cell responses to LCMV that was administered at this time point. To test this hypothesis, mice were infected with wtCVB3, and co-infected with LCMV 2 days later. The frequencies of total $CD8^+$ and $CD4^+$ T cells, and LCMV-specific $CD8^+$ and $CD4^+$ T cell responses, were analyzed in the spleen on day 5 and 7 after LCMV infection. Compared to mice that received LCMV infection alone, the total number of mononuclear cells in the spleen (day 7, Figure 8A) and the frequency of splenic $CD8^+$ T cells (day 5 and 7, Figure 8B) were significantly reduced (~2-fold) in co-infected mice. In contrast, the frequency of $CD4^+$ T cells was not significantly altered by CVB3 co-infection (Figure 8C). The total numbers of $GP_{33}$- and $NP_{396}$-specific $CD8^+$ T cells were significantly lower than in mice infected only with LCMV (Figure 8D & E). Co-infection with wtCVB3 had similar effects on the LCMV-specific $CD4^+$ T cell response; the total number of GP61-specific $CD4^+$ T cells was reduced at both days 5 and 7 after LCMV infection (Figure 8F). The above evaluation of the LCMV-specific T cell responses relied on a functional readout (IFN$\gamma$ production). Thus, it was formally possible that the number of LCMV-induced T cells in CVB3-infected mice was normal, and that the majority of the cells were dysfunctional (IFN$\gamma$-deficient), rendering them undetectable by the above assay. Therefore, we enumerated the cells using appropriate MHC class I tetramers. Compared to mice infected with LCMV alone, the total number of $D^bGP_{33}$ and $D^bNP_{396}$ tetramer$^+CD8^+$ T cells was substantially reduced (>10-fold) in co-infected mice 5 days after LCMV (Figure 8G & H), which parallels the reduction in the total number LCMV-specific IFN-$\gamma^+$ $CD8^+$ T cells (Figure 8D & E). Taken together, these ICCS and tetramer data show that wtCVB3 infection is associated not with enhanced, but rather with significantly weaker $CD8^+$ and $CD4^+$ T cell responses to LCMV, even if LCMV is administered shortly after CVB3 (2 days later) when activated DCs are abundant in the spleen.

The effect of wtCVB3 on the magnitude of the LCMV-specific $CD8^+$ and $CD4^+$ T cell responses varied with, and was dependent upon, two distinct time intervals. *First*, the time allowed to elapse between the CVB3 and LCMV infections. When CVB3 was administered only 2 days prior to LCMV, the responses to LCMV 7 days later were only modestly reduced (Figure 8D–H), while the suppressive effects of CVB3 were much more pronounced when 4 days had elapsed between wtCVB and LCMV infections (Figure 7D & E). *Second*, the time point post-LCMV at which the responses are measured. For $CD8^+$ T cells (Figure 8D, E, G & H) the reduction in LCMV-specific responses was markedly greater at day 5 post-LCMV (~10–20-fold) compared to day 7 (~2–4-fold). A similar observation applies to $CD4^+$ T cells: the total number of GP61-specific $CD4^+$ T cells was strongly reduced 5 days after LCMV (13-fold), but this numerical deficit was partially

restored by day 7, with only a ~3-fold difference between co-infected mice and mice infected with LCMV alone (Figure 8F). Although the effects of wtCVB3 on the magnitude of LCMV-specific T cell responses varies with these time intervals, in all cases the LCMV-specific effector cells appear to be functionally competent to produce IFNγ.

### Conventional dendritic cell numbers are diminished in co-infected mice

To determine if co-infection with wtCVB3 and LCMV led to a similar reduction in cDC numbers as wtCVB3 infection alone, the number of splenic DCs in co-infected mice was assessed at the time points when LCMV-specific T cell responses were measured *ex vivo* (day 5 and 7 post LCMV, Figure 7 & Figure 8). In mice that were infected with wtCVB3 and co-infected with LCMV 3 or 4 days later, the total number of $CD11c^{hi}$ cDCs was significantly diminished 7 days post LCMV infection (10 or 11 days post CVB3) (Figure 9A). Analysis of cDC subsets showed that the total number of $CD8\alpha^+$ and $CD4^+$ cDCs were most profoundly reduced (Figure 9B). Similar results were obtained in mice that were infected with wtCVB3 and co-infected with LCMV 2 days later; DC numbers were significantly reduced at 5 and 7 days post LCMV infection (7 or 9 days post CVB3) (Figure 9C & D). Overall, the number of DCs did not vary substantially between co-infected mice and mice infected with wtCVB3 alone. Rather, cDC numbers were significantly diminished and to a similar extent in both groups of mice (Figure 1, Figure 2, Figure 9).

### The reduced T cell responses to LCMV do not result from lack of replication, and LCMV antigen presentation by splenic APCs from co-infected mice can trigger naïve T cell proliferation

An alternative explanation for the reduced LCMV-specific T cell response in co-infected mice is that CVB3 infection establishes a microenvironment that suppresses LCMV replication, thereby reducing the amount of viral antigen available for priming naïve LCMV-specific T cells. This possibility was assessed in two ways. First, mice were infected with wtCVB3 and then infected with LCMV 2 days later. A control group of mice received only LCMV. Five days after LCMV infection, RNA was isolated from the spleen and liver and the copy number of LCMV genomic S segment RNA was determined by quantitative real time RT-PCR. At this time point, mice infected with LCMV alone had ~$2\times10^7$ genome copies per mg of spleen, and ~$5\times10^6$ per mg of liver; mice that had been infected 2 days previously with wtCVB3 had a similar genome load in the spleen, but significantly elevated (~6-fold) load in the liver (Figure 10). These data suggest that CVB3 does not reduce the ability of LCMV to replicate within co-infected mice. Second, we examined whether splenic APCs from co-infected mice present LCMV antigen in a manner that can drive the proliferation of naïve LCMV-specific $CD8^+$ transgenic T cells. We previously demonstrated that mice infected with rCVB3 expressing LCMV immunodominant epitopes mount very weak endogenous T cell responses *in vivo*, but the capacity of splenocytes from CVB3-infected animals to stimulate naïve T cells *in vitro* was not examined (Kemball *et al.*, 2008; Slifka *et al.*, 2001). Mice were infected with wtCVB3 and, 4 days later (the time point when DCs are strongly affected, Figure 2), the mice received LCMV. Three groups of control mice received CVB3 alone, LCMV alone, or no virus. Splenocytes were harvested from the infected mice at 2 days after LCMV infection and/or 6 days post-CVB3, and were incubated for 2–4 days *in vitro* with CFSE-labeled naïve P14 $CD8^+$ transgenic T cells. Since APCs from the donor P14 spleen could potentially present viral antigens and drive $CD8^+$ transgenic T cell proliferation independently of APCs from virus-infected spleens, P14 $CD8^+$ T cells were purified by magnetic selection (see Materials & Methods), and these enriched $CD8^+$ T cells (93% $CD8^+Thy1.1^+$) were incubated with splenocytes from virus-infected mice. $CD11c^{hi}$ DCs were almost completely absent from this enriched $CD8^+$ T cell fraction (0.03% of selected cells were $CD11c^{hi}Thy1.1^-CD19^-CD49b^-$, data not shown), and therefore a vanishingly small number of DCs in these cultures originated from the P14 donor

mouse. P14 $CD8^+$ T cell proliferation was analyzed by flow cytometry after 2, 3, or 4 days of *in vitro* culture. The vast majority of P14 cells did not divide (remained $CFSE^{hi}$) following stimulation with splenocytes from uninfected mice, or from mice infected with wtCVB3 only (Figure 11A & B). A substantial proportion (~60%) of P14 cells divided (and diluted their CFSE) after 2 days of stimulation with splenocytes from mice infected with LCMV only; by day 3 almost all of the input P14 cells had divided, the majority several times, and they continued to proliferate through day 4 (Figure 11A & B). In contrast, relatively few P14 cells (~20%) had begun to proliferate on day 2 after stimulation with splenocytes from co-infected mice. In addition, prior infection with wtCVB3 altered the CFSE fluorescence profiles observed after 2 days of *in vitro* culture (Figure 11A top row; compare LCMV & co-infected panels): although, in both cases, the maximum number of observed divisions was 4, many more cells had undergone 1–4 divisions in response to splenocytes from mice infected with LCMV alone, compared to splenocytes from co-infected mice. Thus, wtCVB3 co-infection appears to diminish the division of naïve LCMV-specific $CD8^+$ T cells *in vitro*, paralleling what we have observed *in vivo*. However, as we have also observed *in vivo* (Figure 8), the magnitude of the effect diminishes with time; after 3 days of stimulation by splenocytes from co-infected mice, the majority of naïve P14 cells in co-infected culture wells had proliferated, and almost all of the sensor cells had divided by day 4 (Figure 11A & B). To determine if P14 T cell proliferation increased when the level of viral antigen presentation by co-infected splenocytes was artificially increased, we setup an additional group of cultures in which P14 cells were incubated with co-infected splenocytes together with $GP_{33–41}$ peptide. In these wells, a greater percentage of P14 cells (~70%) had divided after 2 days of culture, and this was similar to the proportion of P14 cells that divided following stimulation with splenocytes from mice infected with LCMV alone (Figure 11A & B). P14 cells stimulated with co-infected splenocytes + peptide continued to divide further by day 4 of culture. Thus, we conclude that the weaker proliferation of P14 cells in co-infected (no peptide) cultures on day 2 most likely resulted from a lower level of LCMV antigen presentation and/or fewer APCs presenting viral antigens to T cells; and that this deficiency could be overcome by provision of abundant peptide antigen. In support of this hypothesis, flow cytometric analysis of the stimulator splenocytes from the various groups showed that, when added to the wells at the beginning of the culture, the frequency of $CD8\alpha^+CD11c^{hi}$ DCs was substantially lower in co-infected mice compared to mice infected with LCMV alone (Figure 11C). In summary, these data show that, in co-infected mice, endogenous LCMV antigen is presented sufficiently well to trigger naïve $CD8^+$ T cell proliferation *in vitro*. However, T cell division is delayed compared to that observed with LCMV-only stimulator cells; this delay appears to result, in part, from a lower level of viral antigen presentation and/or fewer APCs; and it can be overcome by the addition of exogenous $GP_{33–41}$ peptide to co-infected cultures.

## Purified dendritic cells from LCMV-infected or co-infected mice are similarly capable of stimulating T cell proliferation in vitro

The data presented in Figure 11 show that splenic APCs from co-infected mice can stimulate naïve $CD8^+$ T cell proliferation *in vitro*, although the functionality of DCs was not assessed independently of other splenic APCs. It is unclear whether the delay in T cell expansion *in vitro* is due to decreased functionality of DCs or due to a reduction in their numbers alone. In order to isolate DC function from that of other APCs, groups of mice were infected with wtCVB3 and/or LCMV as in Figure 11, spleens were harvested (and pooled within mouse groups), and $CD11c^+$ DCs were purified by magnetic selection. Flow cytometric analysis of these purified DCs populations showed a lower frequency of $CD8\alpha^+CD11c^{hi}$ DCs in co-infected mice compared to mice infected with LCMV alone (Figure 12C), in agreement with the analysis of non-purified DCs (Figure 11C). An equal number of purified DCs from each group were incubated with purified, CFSE-labeled, P14 T cells for 2–4 days *in vitro*. The

majority of P14 cells did not divide (remained $CFSE^{hi}$) following stimulation with DCs from uninfected mice, or from mice infected with wtCVB3 only (Figure 12A & B). A substantial proportion (~30%) of P14 cells divided after 2 days of stimulation with DCs from mice infected with LCMV only; by day 3 most of the input P14 cells had divided, the majority several times, and they continued to proliferate through day 4 (Figure 12A & B). A similar response by P14 cells was observed using DCs from co-infected mice, and the kinetics of P14 cell division were comparable in wells containing DCs from co-infected mice or mice infected with LCMV alone (Figure 12A & B). To determine if P14 T cell proliferation increased when the level of viral antigen presentation by co-infected DCs was artificially increased, we setup an additional group of cultures in which P14 cells were incubated with $GP_{33–41}$ peptide-pulsed, purified DCs from co-infected mice. In these wells, the vast majority of P14 cells (~95%) had divided after 2 days of culture, and continued to divide further on day 3 and 4 (Figure 12A & B). Taken together, these data show that when equal numbers of purified DCs (from LCMV-only and co-infected mice) are used as stimulators, both populations are similarly capable of stimulating in vitro T cell proliferation. Therefore, the delay in T cell division following stimulation with co-infected splenocytes (Figure 11A & B) is most likely due to the reduced number of DCs present in the culture wells (compared to splenocytes from mice infected with LCMV alone), rather than a decrease in DC functionality.

## Discussion

*In vitro* studies have suggested that enteroviruses utilize strategies that impair the ability of DCs to trigger adaptive immunity, by inhibiting protein synthesis within DCs, and by limiting cellular maturation, antigen presentation, and proinflammatory cytokine secretion. However, it is not known whether picornaviruses exert similar effects on DCs *in vivo*, or if other effects of virus infection also modulate the stimulatory capacity of DCs. Although DC infection by coxsackievirus has been reported, the extent to which it occurs *in vivo*, and the level of protein expression in infected DCs, was unknown. In the present study, we evaluated the effects of wtCVB3 on DCs *in vivo* and *in vitro*, and we make several novel observations: first, viral protein synthesis is extremely limited in DCs and the relative frequency of infected DCs is very low, both *in vitro* and *in vivo*. Second, wtCVB3 nevertheless substantially affects DCs and reduces their numbers more profoundly than in other well-characterized viral systems. Third, the severe reduction in $CD8\alpha^+$ cDCs is associated with a reduced ability of the host to mount T cell responses to a subsequent viral infection. Finally, DCs obtained from wtCVB3-infected mice do present antigen in a manner that can trigger naïve $CD8^+$ T cell responses, but the T cell responses are delayed, both *in vivo* and *in vitro*.

CVB3 does not establish a productive infection in murine DCs (Weinzierl *et al.*, 2008b), and cannot replicate in human DCs upon entry via phagocytosis (Schulte *et al.*, 2010). However, a recent study found that murine DCs can endocytose CVB3 virions, and reported that DCs isolated from infected mice contain positive and negative strand viral RNA (Weinzierl *et al.*, 2008b). Thus, we considered the possibility that DCs may be non-productively infected by CVB3 *in vivo*; if viral proteins were generated in sufficient abundance within infected DCs, they might lead to cell death and/or inhibit the presentation of MHC class I-restricted CVB3 epitopes, thereby contributing to the weak primary CVB3-specific T cell response, and to the reduction in LCMV-specific T cell responses reported herein. However, very few virus-infected DCs expressing DsRed protein were detected in the spleen and pancreatic lymph nodes of DsRed-CVB3-infected mice (Figure 5). In addition, *in vitro* exposure of murine DCs to CVB3 at high multiplicity did not lead to viral protein expression (VP1 or GFP) at a level detectable by flow cytometry (Figure 6A), and the cells did not exhibit significant changes in their surface expression of MHC class I & II and CD86 (Figure 6B and data not

shown). Furthermore, CVB3 did not cause detectable cytopathic effects and, as others have reported, productive infection did not take place. We cannot exclude the possibility that a small subset of DCs is infected by CVB3 *in vivo* and that, in these cells, direct presentation of MHC class I-restricted antigens is compromised by the virus; but these data suggest that CVB3 may elude naïve $CD8^+$ T cells in large part by the simple expedient of avoiding DCs, rather than by inhibiting antigen presentation within these key APCs. However, this raises another issue: even if the virus does not infect DCs, one would expect that CVB-encoded epitopes would be presented to naïve $CD8^+$ T cells by DCs that are specialized for cross presentation / cross-priming ($CD8^+CD205^+$ DCs). Our previous study suggested that this alternate mode of entry to the MHC class I pathway does not operate efficiently during CVB3 infection, but the molecular basis for the apparent failure of cross-priming in CVB3-infected mice has not been determined (Kemball *et al.*, 2009). One possible explanation is that these DCs are indirectly affected by CVB3 infection. By this hypothesis, CVB3 not only evades DCs by failing to infect them, it also disrupts – probably by indirect means – the DCs that might otherwise present viral epitopes for cross-priming.

We found that, despite its inability to infect DCs in a widespread fashion, wtCVB3 causes a rapid and profound reduction in DC numbers (Figure 1), and alters the relative proportions of the various cDC subsets (Figure 2). From the data in Figure 5 and Figure 6, these changes are unlikely to be caused by direct infection of DCs; rather, the CVB3-related reduction in DC numbers is more likely to be mediated indirectly. Although changes in DC abundance and heterogeneity have been observed in other viral infection models, our findings suggest that the reduction in cDCs in CVB3-infected mice is more profound compared to other virus infections. For example, the decline in numbers of splenic $CD8\alpha^+$ and $CD4^+$ cDCs is more modest following LCMV Armstrong infection (2–3 fold reduction by day 3 p.i.), and cDC numbers remain stable (or increase slightly) following murine cytomegalovirus and γ-herpesvirus 68 infections (Dalod *et al.*, 2003; Montoya *et al.*, 2005; Weslow-Schmidt *et al.*, 2007). The reduction in cDCs that follows LCMV infection is mediated in part by type I IFN signaling (Montoya *et al.*, 2005). Type I IFN levels peak in the serum of CVB3- and LCMV-infected mice at a similar time point (24–48 hrs p.i.) (Huhn *et al.*, 2010; Lee *et al.*, 2009; Wang *et al.*, 2010; Zuniga *et al.*, 2008), so we speculate that the reduction of cDCs in CVB3-infected mice may be mediated by type I IFNs; experiments to evaluate this hypothesis are particularly challenging in the CVB model because, in the absence of type I IFN signaling, CVB infection is invariably lethal within 2–4 days (ref Wessely *et al.*, 2001, and Kemball, Flynn & Whitton, unpublished data).

pDC accumulation has been observed in lymphoid and non-lymphoid tissues during virus infections in mice and humans, and the recruitment of pDCs can either positively or negatively affect the antiviral immune response (Swiecki and Colonna, 2010a). Following CVB3 infection, we found that the total number and frequency of pDCs increases dramatically between day 4 and day 6 days p.i. (Figure 1 D & F). In addition, flow cytometric analysis of splenic pDCs in virus-infected mice (from day 4 onward) showed that these cells are considerably larger in size compared to pDCs in uninfected animals, and suggests that these cells have been activated, and are blasting and/or mature (data not shown). The dramatic increase in pDC numbers cannot be attributed to activated T cells that up-regulated the DC marker CD11c, because our pDC gating strategy excluded cells that expressed the T cell marker CD3 (Figure 1F). During CVB3 infection, pDC activation appears to require engulfment of virus-antibody complexes, and results in TLR-7-dependent production of type I IFN (Wang *et al.*, 2007). Thus, the antiviral effects of pDCs in response to wtCVB3 may be delayed until antiviral antibodies have developed, and we speculate that the dramatic increase in pDC numbers at day 6 is temporally associated with the emergence of virus-specific antibodies that facilitate pDC activation. CVB3 antibodies are detectable by ~day 4 p.i. (Henke *et al.*, 1995) which, as shown in Figure 1D, coincides with an increase in

the number of pDCs in the spleen of infected mice. Unlike mature cDCs, activated pDCs do not down-regulate MHC class II ubiquitination and turnover, and as a result new MHC class II-peptide complexes are continually generated following pDC maturation (Villadangos and Young, 2008; Young *et al.*, 2008). Therefore, we propose that, at ~day 4 and beyond, when cDCs are fewer in number, pDCs may play a role in CVB3 immunity by maintaining MHC class II presentation of CVB3 epitopes to CVB3-specific $CD4^+$ T cells.

The loss of cDCs that occurs at 3–4 days after wtCVB3 infection is striking, and prompted us to question whether wtCVB3 infection diminishes the ability of an infected animal to mount T cell responses to a secondary infection. We have previously demonstrated that rCVB3 infection has no such effect (Kemball *et al.*, 2009), but rCVB3 are generally attenuated *in vivo*, and we considered it vital to evaluate the effects of the wt virus. In stark contrast to rCVB3, we found that wtCVB3 infection dampened $CD8^+$ and $CD4^+$ T cell responses to subsequent LCMV infection; the magnitude of LCMV-specific T cell responses at day 7 post LCMV were considerably reduced (≥10-fold) in mice that had received wtCVB3 4 days prior to LCMV (Figure 7D & E). This suppressive effect of wtCVB3 infection was rapid, and could be observed even when LCMV was administered only 2 days after CVB3; the total number of LCMV-specific T cells was strongly reduced 5 days later. However, this rapid effect was not absolute because, by day 7 post LCMV, there was only a modest difference in the magnitude of the T responses in co-infected mice compared to those in mice infected with LCMV alone (Figure 8D–F). Thus, wtCVB3 infection delays LCMV-specific T cell expansion, but does not prevent it. Furthermore, dysfunctional cells were not identified in co-infected mice (Figure 8D, E, G, & H), indicating that, although slower to accumulate, the responding effector T cells in these mice are functionally competent and produce antiviral cytokines. Thus, wtCVB3 infection dampens, but does not ablate, host $CD8^+$ T cell immunity.

The most obvious explanation for the lower LCMV-specific T cell responses in co-infected mice invokes the wtCVB3-related changes in DC quantity and quality. Our analysis of cDC numbers in co-infected mice, and mice infected with wtCVB3 alone, showed that these cells were significantly diminished and to a similar extent in both groups ((Figure 1, Figure 2, Figure 9). It is easy to imagine how the substantial reduction in DC numbers caused by wtCVB3 at 3 & 4 days p.i. (Figure 1, Figure 2) might diminish the host's ability to mount primary T cell responses to subsequent LCMV infection, and our *in vitro* stimulation data (Figure 11) are consistent with this hypothesis. Compared with splenocytes from mice infected with LCMV alone, the frequency of $CD8\alpha^+$ DCs was substantially lower in co-infected stimulator splenocytes (day 2 post LCMV/day 6 post CVB3, data not shown), and these "$CD8\alpha^+$ DC-depleted" splenocytes induced fewer LCMV-specific T cells to proliferate after 2 days of *in vitro* culture (Figure 11C). In contrast, when equal numbers of purified DCs (from LCMV-only and co-infected mice) were used as stimulators, both populations were similarly capable of stimulating T cell proliferation (Figure 12A & B). Together, these data suggest that the delayed T cell responses to co-infected splenocytes *in vitro* are due to a reduction in DC numbers rather than a decrease in DC functionality. The impact of these quantitative differences may be amplified by the qualitative changes in the APCs that are rapidly induced by wtCVB3 infection *in vivo*. Qualitative changes (e.g., cell maturation) in $CD8\alpha^+$ DCs occur as early as day 2 p.i. (Figure 4), preceding their numerical collapse (Figure 2D & E), and we speculate that these changes may contribute both to the delayed T cell response when LCMV is administered at this time point (Figure 8) and to the delayed T cell response that is observed *in vitro* (Figure 11). However, qualitative changes alone may not have irredeemable effects because, in mice infected with LCMV at 2 days after wtCVB3 infection, the magnitude of the LCMV-specific $CD8^+$ T cell response in these mice is only modestly reduced 7 days later (Figure 8); similarly, P14 T cell proliferation *in vitro* appears to progress normally by day 3–4 (Figure 11). Based on these findings we

speculate that, in mice that receive LCMV shortly after CVB3 (2 days later, Figure 8), the kinetics of LCMV-specific T cell expansion are altered because wtCVB3 infection reduces DC quality, delaying (but not aborting) the expansion of LCMV-specific T cells. If the interval between these infections is increased (e.g. if LCMV is given 3 or 4 days after CVB3), both quality and quantity are markedly reduced, thereby amplifying the suppressive effect of wtCVB3 on the LCMV T cell response. In contrast, if LCMV is given 3 days after rCVB3 infection, LCMV-specific T cell responses are enhanced, which suggests that the less virulent recombinant virus does not exert these suppressive effects on DCs; rather, rCVB3 infection appears to establish a microenvironment that is capable of promoting strong T cell responses against a subsequent virus infection (Kemball *et al.*, 2009). We considered the possibility that the weaker LCMV-specific T cell response in CVB3-infected mice might result from a reduced level of LCMV antigen, perhaps because LCMV replication was suppressed by ongoing host responses to the CVB3 infection. However, our quantitative assessment of LCMV genomes in the spleen and liver suggests that LCMV replication is not limited by CVB3 co-infection. On the contrary, the number of LCMV genomes in these organs was similar to, or slightly greater than, the number measured in mice infected with LCMV alone (Figure 10). Indeed, our finding that LCMV genome copy numbers were significantly higher in the livers of co-infected mice, which lack strong LCMV-specific T cell responses, is consistent with the fact that control of LCMV is T cell-dependent (Ahmed *et al.*, 1988; Ahmed *et al.*, 1984; Jamieson *et al.*, 1987). It is unclear why LCMV replication is not inhibited by the innate immune response to CVB3. Levels of type I IFN peak in the serum and pancreas of CVB3-infected mice at day 2 p.i. (the time point at which mice were co-infected with LCMV, Figure 8), but this increase is not observed in the liver (Huhn *et al.*, 2010; Wang *et al.*, 2010). Therefore, it is conceivable that LCMV may escape the effects of CVB3-induced type I IFN in some sites including the liver and spleen. Furthermore, CVB3 can disrupt type I IFN signaling *in vitro* by cleaving the innate immune adaptor molecules MAVS and TRIF, and we speculate that antagonism of these signaling pathways by CVB3 *in vivo* could minimize the effects of type I IFN on concurrent LCMV replication (Mukherjee *et al.*, 2011).

The effects of CVB3 on DCs, and in particular $CD8^+CD205^+$ DCs, may contribute to our previous findings that $CD8^+$ T cell responses to CVB3 are barely detectable (Kemball *et al.*, 2009; Kemball *et al.*, 2008; Slifka *et al.*, 2001). However, we feel that additional factors must play a role, for several reasons. *First*, activation of DCs is known to decrease their ability to cross-prime naïve virus-specific T cells (Segura and Villadangos, 2009; Wilson *et al.*, 2006; Young *et al.*, 2007); consequently, cross-priming is thought to occur very soon after the onset of infection, when naïve $CD8^+$ T cells interact briefly with immature antigen-bearing DCs (Hickman *et al.*, 2008; Kastenmuller *et al.*, 2010; Norbury *et al.*, 2002). One would expect that CVB3 proteins synthesized in the first hours p.i. would gain access to, and be cross-presented by, immature DCs, prior to their being activated by the infection. This appears not to occur. *Second*, we show here that a wtCVB3-infected host remains capable of mounting a strong (albeit slightly delayed) response as late as 2 days after wtCVB3 infection (Figure 8). At this time point, $CD8\alpha^+$ DCs are numerous, and wtCVB3 has replicated to high titers (Figure 5A), so viral proteins are abundant, yet mice do not develop a readily-detectable CVB3-specific $CD8^+$ T cell response (Kemball *et al.*, 2009); this suggests that the existing $CD8\alpha^+$ DCs do not effectively cross-prime in these wtCVB-infected mice. *Third*, even when DCs are largely depleted by wtCVB3 infection (day 4 p.i.) the host remains capable of mounting a detectable response to LCMV. We cannot exclude other, DC-independent, explanations that may contribute to the weak primary T cell response to CVB, and for the diminished LCMV-specific T cell response in wtCVB3-infected mice. For example, somewhat counter-intuitively, many viruses cause a rapid but transient lymphopenia (Bautista *et al.*, 2003; Díaz-San Segundo *et al.*, 2006; Dietz, Jr. *et al.*, 1979; Geisbert *et al.*, 2000; Grubman *et al.*, 2008; Nfon *et al.*, 2010; O'Donnell and Carrington,

2002; Okada *et al.*, 2000; Peacock *et al.*, 2003); the effect, which is mediated by interferons (Kamphuis *et al.*, 2006; Schattner *et al.*, 1983), has been shown to occur during enteroviral infections (Bautista *et al.*, 2003; Nfon *et al.*, 2010) and we have observed it in mice infected with wtCVB3 (Althof & Whitton, unpublished).

In conclusion, our evaluation of the effects of wtCVB3 on DCs *in vitro* and *in vivo* reveals that the infection dramatically alters the abundance, heterogeneity, and immunostimulatory capacity of conventional dendritic cells. These changes are unlikely to be the result of direct infection of DCs by CVB3, and instead the virus appears to induce DC maturation and decay in an indirect manner. The loss of $CD8\alpha^+$ DCs may deprive the host of the most potent inducers of virus-specific T cell responses, and other effects on cDCs, e.g., on activation/maturation, may augment the immunoevasive effects of CVB3 and related enteroviruses *in vivo*. These features also may weaken the host's capacity to mount T cell responses to a secondary virus infection.

## Materials & Methods

### Mice, viruses, and infections

C57BL/6J mice were purchased from The Scripps Research Institute (TSRI) breeding facility. P14/Thy1.1 TCR transgenic mice specific for the H-$2D^b$ restricted LCMV epitope $GP_{33–41}$ (Pircher *et al.*, 1990) were bred and maintained by our laboratory as described (Whitmire *et al.*, 2006; Whitmire *et al.*, 2008). This study was carried out in accordance with the recommendations in the Guide for the Care and Use of Laboratory Animals of the National Institutes of Health. All experimental procedures with mice were reviewed and approved by TSRI Animal Care and Use Committee. The wtCVB3 used in these studies is a plaque-purified isolate (designated H3) of the myocarditic Woodruff variant of CVB3 (van Houten *et al.*, 1991). Plasmid pH3, encoding a full length infectious clone of this virus (Knowlton *et al.*, 1996), was provided by Kirk Knowlton (University of California, San Diego, CA). Recombinant CVB3 encoding eGFP or DsRed were generated as described previously (Feuer *et al.*, 2002; Tabor-Godwin *et al.*, 2010). wtCVB3, eGFP-CVB3, and DsRed-CVB3 were grown in HeLa cells, and virus stocks were generated as described previously (Harkins *et al.*, 2005). Naïve adult male C57BL/6J mice were inoculated i.p. with $1\times10^3$ PFU of wtCVB3, $1\times10^7$ PFU of DsRed-CVB3, or $2\times10^5$ PFU of LCMV Armstrong. To confirm CVB3 infection, the virus titer in the feces was determined on day 2 post infection, as described previously (Kemball *et al.*, 2009). Pancreas was isolated from wtCVB3-infected mice, weighed, and homogenized in 1 ml DMEM, and the titer of infectious virus in the lysate was determined. Plaque assays were performed on subconfluent HeLa cell monolayers, as described previously (Hunziker *et al.*, 2007), and the virus titer (PFU/g) was calculated for each sample.

### Lymphocyte isolation

Spleens and pancreatic lymph nodes were minced and digested with collagenase D (1 mg/ml, Roche) and DNase I (20 μg/ml, Roche) for 30 min at 37°C, and then filtered through a 70 μm cell strainer (BD Biosciences) to generate a single cell suspension. Red blood cells were lysed with 0.83% $NH_4Cl$.

### Isolation and culture of bone marrow-derived dendritic cells

Bone marrow was flushed from the femurs and tibiae of C57BL/6J mice using cold DPBS (Invitrogen). Marrow was passed repeatedly through an 18-gauge needle and then filtered through a 70 μm cell strainer to generate a single cell suspension. Viable cells were separated from dead cells and erythrocytes using Lympholyte-M (Cedarlane Labs), according to the manufacturer's instructions. Cells were setup in 24-well plates ($1–2\times10^6$

cells/well) in 1 ml of BMDC culture media (RPMI containing 10% FBS, L-glutamine, 2-mercaptoethanol, penicillin/streptomycin, sodium pyruvate, and HEPES) with recombinant murine GM-CSF (50 ng/ml, Peprotech), and cultured for 6–10 days before use. On day 2, 700 ul of media was removed from each well and replaced with fresh media + GM-CSF. On day 3, the entire volume of media was removed from the wells, then the cells were gently washed with 500 ul fresh media (to remove residual non-adherent cells), and 1 ml of culture media + GM-CSF was added to the wells. Thereafter, cells were fed daily with 1 ml culture media + GM-CSF.

### In vitro antigen presentation assay

Transgenic T cells were used to detect the presentation of LCMV antigen by splenocytes isolated from virus-infected mice. To prepare these indicator cells, $CD8^+$ T cells were purified from the spleens of P14/Thy1.1 TCR transgenic mice by MACS separation (negative selection) using a mouse $CD8\alpha^+$ T cell Isolation Kit II (Miltenyi Biotec), following the manufacturer's instructions. The purity of enriched $CD8^+$ T cells (93%) and the frequency of P14 transgenic T cells ($CD8^+V\alpha2^+$) were determined by flow cytometry. P14 cells were labeled with 3 μM CFSE. Single cell suspensions of spleens from virus-infected mice were prepared (see Lymphocyte isolation, above), and $10^6$ stimulator spleen cells were incubated with $5\times10^4$ P14 transgenic T cells per well in 96-well flat bottom plates containing 0.2 ml culture media (RPMI containing 10% FBS, 50 μM 2-mercaptoethanol, and penicillin/streptomycin). One set of cultures included P14 cells, splenocytes from co-infected mice, and 1 μM LCMV $GP_{33–41}$ peptide. Duplicate cultures were setup for each sample. Cells were fed on day 2 and 3 of culture; ~1/2 the volume of media from each well was removed, and replaced with 100 μl fresh culture media. Wells were harvested after 2, 3, and 4 days of culture, and transgenic T cell proliferation was determined by flow cytometry.

To analyze antigen presentation by DCs, these cells were enriched from the spleens of virus-infected mice by MACS separation (positive selection) using mouse CD11c microbeads (Miltenyi Biotec), following the manufacturer's instructions. The spleens within each mouse group (3–6 mice/group) were pooled before MACS separation. $6\times10^4$ $CD11c^{hi}$ cells were incubated with $1.2\times10^5$ CFSE-labeled P14 cells per well. In one set of cultures, DCs from co-infected mice were pulsed with 1 μM $GP_{33–41}$ peptide for 30 min in 96-well culture wells ($1.2\times10^5$ cells/well), then washed to remove unbound peptide, and incubated with P14 cells. Triplicate cultures were setup for each group. Wells were harvested after 2, 3, and 4 days of culture, and transgenic T cell proliferation was determined by flow cytometry.

### Flow cytometry

Cells were incubated with Fc receptor antibody (FcBlock, BD Biosciences) in PBS containing 2% FBS and 0.1% sodium azide (FACS buffer) for 10 min on ice. Cells were then surface stained with fluorochrome-conjugated antibodies and/or MHC class I tetramers (NIH Tetramer Core Facility, Atlanta, GA) in FACS buffer for 30 min on ice, and washed 2X in FACS buffer. Following the surface staining, some samples were stained with eFluor780-conjugated fixable viability dye (eBioscience) following the manufacturer's instructions, in order to identify dead cells during flow cytometry and exclude them from our analyses. Samples were fixed in PBS containing 1% paraformaldehyde and acquired on a FACSCalibur or LSR-II (BD Biosciences). Data were analyzed with FlowJo software (TreeStar).

For intracellular cytokine staining of splenocytes, $2\times10^6$ splenocytes were incubated for 5 hrs in 96-well plates in 0.2 ml/well RPMI containing 10% FBS, 50 μM 2-mercaptoethanol, penicillin/streptomycin, GolgiPlug (BD Biosciences), and synthetic peptides (1 μM LCMV $GP_{33–41}$ or $NP_{396–404}$, 10 μM $GP_{61–80}$). After stimulation, cells were incubated with

FcBlock, stained with CD8 or CD4 antibodies as described above, then stained for intracellular IFNγ with the Cytofix/Cytoperm kit (BD Biosciences). The total number of epitope-specific cytokine-producing T cells was determined by subtracting unstimulated cytokine$^+$ T cells (no peptide) from peptide-stimulated cytokine$^+$ T cells.

For intracellular staining of CVB3-infected primary BMDCs and cell lines [including DC2.4 cells (kindly provided by Ken Rock, University of Massachusetts) and HeLa cells], cells were detached from tissue culture wells by forceful pipetting or treatment with versene (Invitrogen), and then washed and resuspended in FACS buffer. Cells were permeabilized with the Cytofix/Cytoperm kit, and then stained with VP1 antibody in Permwash for 30 min on ice.

The following antibodies were used for the flow cytometric analyses described above. Fluorochrome-conjugated CD11c (clone N418), CD11b (clone M1/70), CD3ε (clone 145-2C11), CD19 (clone 6D5), CD49b (clone DX5), CD8α (clone 53-6.7), CD4 (clone RM4-5 and GK1.5), Thy1.1 (clone HIS51), Thy1.2 (clone 53-2.1), Vα2 (clone B20.1), MHC class I (clone 28-14-8), MHC class II (clone M5/114.15.2), CD40 (clone HM40-3), CD80 (clone 16-10A1), CD86 (clone GL1), IFNγ (clone XMG1.2), and isotype control antibodies were purchased from eBioscience or BioLegend. CD205 (clone NLDC-145) and mPDCA-1 (clone JF05-1C2.4.1) antibodies were purchased from Miltenyi Biotec. VP1 antibody (clone 5-D8/1) was purchased from Leica Microsystems as a lyophilized tissue culture supernatant. The antibody was reconstituted in water, column purified by TSRI Antibody Core Facility, and conjugated to Alexa Fluor 647 using a Molecular Probes monoclonal antibody labeling kit (Invitrogen).

### Vibratome sectioning and confocal microscopy

Mice were perfused with DPBS, and the pancreas was harvested and fixed in buffered zinc formalin (Z-FIX, Anatech Ltd.) at RT for 5 days. The fixative was replaced with PBS and tissues were preserved at 4°C. Sections of pancreas (80 μm) were cut with a VT1000 S vibratome (Leica Microsystems, Inc.). Free floating sections were washed 3 times in PBS and permeabilized in PBS with 0.5% Triton X-100 for 30 min at RT. Next, the sections were washed twice in PBS with 0.1% Triton X-100 and then incubated with Alexa Fluor 488-conjugated phalloidin (Invitrogen) in PBS with 0.1% Triton X-100 overnight at 4°C (to label F-actin). After incubation, the sections were washed twice in PBS with 0.1% Triton X-100 and then 3 times in PBS. Lastly, sections were stained with Hoechst 33342 (Invitrogen) in PBS for 30 min at RT (to label nuclei) and then washed 3 times in PBS and mounted on glass slides with ProLong Gold mounting medium (Invitrogen). Three color images were captured using a LSM 710 laser scanning confocal microscope equipped with ZEN software (Carl Zeiss, Inc.). Representative regions within each vibratome section of pancreas were scanned at ×40 magnification as serial 8-bit optical sections with 0.5 μm interval step sizes (512 by 512 image size). Images were analyzed with Imaris software (BitPlane, Inc.) and maximum projected for presentation using the Easy 3D function.

### Quantitative real time PCR

Spleen and liver samples were collected and immediately stored in RNAlater stabilization reagent (Qiagen). RNA was isolated from these organs with an RNeasy mini kit (Qiagen), following the manufacturer's instructions, and genomic LCMV RNA (present in mature virions) was quantitated as follows. A reverse transcription (RT) primer ($^5$'CAGGGTGCAAGTGGTGTGGTAAGA$^3$') complementary to residues 2865 to 2842 of the viral S segment genomic RNA was synthesized, and used in an RT reaction together with 1/10$^{th}$ of the total RNA sample, MultiScribe RT, 10× PCR Buffer II, $MgCl_2$, RNAse Inhibitor, and GeneAmp dNTP Mix (all from Applied Biosystems). Additional control

reactions were setup that omitted RT ("no RT"). The RT reaction was carried out in a thermocycler as follows: 25°C for 10 min, 48°C for 30 min, 95°C for 5 min. Next, Taqman quantitative real time PCR was performed using the following primers and probe: forward primer (Arm S 2275+), $^{5}$'CGCTGGCCTGGGTGAAT$^{3}$'; reverse primer (Arm S 2338-), $^{5}$'ATGGGAAAACACAACAATTGATCTC$^{3}$', Taqman FAM/MGB-labeled probe, $^{5}$'TTGCTGCAGAGCTTA$^{3}$'. PCR reactions contained primers & probe, TaqMan Universal PCR Master Mix (No AmpErase UNG, Applied Biosystems), and 1/10$^{th}$ of the total cDNA. Quantitative analysis of viral RNA was carried out using a BioRad iQ5 real time PCR system in 96-well optical reaction plates heated to 95°C for 10 min, followed by 40 cycles of: denaturation at 95°C for 15 s and annealing and extension at 60°C for 1 min. All samples were evaluated in triplicate amplification reactions. Dilutions of the p-T7-S plasmid (encoding the S segment of the LCMV Armstrong genome, kindly provided by Juan Carlos de la Torre, TSRI) were analyzed (in quadruplicate) to generate a standard curve. The standard curve was based on threshold cycle (CT) values, and CT values from tissue samples were compared to the standard curve to determine viral RNA copy numbers. The limit of detection of this assay is 5 copies of viral RNA/reaction. Values are expressed as the average number of LCMV genomes per mg tissue; these were determined by calculating the total number of LCMV genomes per RNA sample, divided by the sample weight.

### Statistical analyses

Statistical significance was determined by an unpaired two-tailed t-test, or by one-way ANOVA with Tukey's post hoc test (GraphPad Prism software). A p value $<0.05$ was considered statistically significant.

## Acknowledgments

We thank Annette Lord and Sheila Silverstein for excellent secretarial support. We also thank the NIH Tetramer Core Facility for providing MHC class I tetramers, and Dr. Ken Rock (University of Massachusetts) for providing the DC2.4 cell line. This work was supported by NIH grants AI042314 and HL093177 (to J.L.W.); T32 NS41219 and F32 AI078660 (to C.C.K.); T32 HL007195-34 (to M.P.H.), and F32 AI056827, P20 RR021905, and R21 AI088059 (to J.B.). This is manuscript number 21350 from the Scripps Research Institute.

## References

Ahmed R, Butler LD, Bhatti L. T4$^{+}$ T helper cell function in vivo: differential requirement for induction of antiviral cytotoxic T-cell and antibody responses. J. Virol. 1988; 62:2102–2106. [PubMed: 2966865]

Ahmed R, Salmi A, Butler LD, Chiller JM, Oldstone MBA. Selection of genetic variants of lymphocytic choriomeningitis virus in spleens of persistently infected mice: role in suppression of cytotoxic T lymphocyte response and viral persistence. J. Exp. Med. 1984; 160:521–540. [PubMed: 6332167]

Bautista EM, Ferman GS, Golde WT. Induction of lymphopenia and inhibition of T cell function during acute infection of swine with foot and mouth disease virus (FMDV). Vet. Immunol. Immunopathol. 2003; 92:61–73. [PubMed: 12628764]

Belz GT, Shortman K, Bevan MJ, Heath WR. CD8α$^{+}$ dendritic cells selectively present MHC class I-restricted noncytolytic viral and intracellular bacterial antigens in vivo. J. Immunol. 2005; 175:196–200. [PubMed: 15972648]

Choe SS, Dodd DA, Kirkegaard K. Inhibition of cellular protein secretion by picornaviral 3A proteins. Virology. 2005; 337:18–29. [PubMed: 15914217]

Crocker SJ, Frausto RF, Whitmire JK, Benning N, Whitton JL. Amelioration of coxsackievirus B3-mediated myocarditis by inhibition of tissue inhibitors of matrix metalloproteinase-1. Am. J. Pathol. 2007; 171:1762–1773. [PubMed: 18055551]

Daley AJ, Isaacs D, Dwyer DE, Gilbert GL. A cluster of cases of neonatal coxsackievirus B meningitis and myocarditis. J. Paediatr. Child Health. 1998; 34:196–198. [PubMed: 9588649]

Dalod M, Hamilton T, Salomon R, Salazar-Mather TP, Henry SC, Hamilton JD, Biron CA. Dendritic cell responses to early murine cytomegalovirus infection: subset functional specialization and differential regulation by interferon alpha/beta. J. Exp. Med. 2003; 197:885–898. [PubMed: 12682109]

Deitz SB, Dodd DA, Cooper S, Parham P, Kirkegaard K. MHC I-dependent antigen presentation is inhibited by poliovirus protein 3A. Proc. Natl. Acad. Sci. U. S. A. 2000; 97:13790–13795. [PubMed: 11095746]

Díaz-San Segundo F, Salguero FJ, de Avila A, de Marco MM, Sanchez-Martin MA, Sevilla N. Selective lymphocyte depletion during the early stage of the immune response to foot-and-mouth disease virus infection in swine. J. Virol. 2006; 80:2369–2379. [PubMed: 16474143]

Dietz WH Jr, Peralta PH, Johnson KM. Ten clinical cases of human infection with venezuelan equine encephalomyelitis virus, subtype I-D. Am. J. Trop. Med. Hyg. 1979; 28:329–334. [PubMed: 222156]

Dodd DA, Giddings TH Jr, Kirkegaard K. Poliovirus 3A protein limits interleukin-6 (IL-6), IL-8, and beta interferon secretion during viral infection. J. Virol. 2001; 75:8158–8165. [PubMed: 11483761]

Dominguez PM, Ardavin C. Differentiation and function of mouse monocyte-derived dendritic cells in steady state and inflammation. Immunol. Rev. 2010; 234:90–104. [PubMed: 20193014]

Dudziak D, Kamphorst AO, Heidkamp GF, Buchholz VR, Trumpfheller C, Yamazaki S, Cheong C, Liu K, Lee HW, Park CG, Steinman RM, Nussenzweig MC. Differential antigen processing by dendritic cell subsets in vivo. Science. 2007; 315:107–111. [PubMed: 17204652]

Feuer R, Mena I, Pagarigan RR, Slifka MK, Whitton JL. Cell cycle status affects coxsackievirus replication, persistence, and reactivation*in vitro* . J. Virol. 2002; 76:4430–4440. [PubMed: 11932410]

Feuer R, Pagarigan RR, Harkins S, Liu F, Hunziker IP, Whitton JL. Coxsackievirus targets proliferating neuronal progenitor cells in the neonatal CNS. J. Neurosci. 2005; 25:2434–2444. [PubMed: 15745971]

Geisbert TW, Hensley LE, Gibb TR, Steele KE, Jaax NK, Jahrling PB. Apoptosis induced in vitro and in vivo during infection by Ebola and Marburg viruses. Lab Invest. 2000; 80:171–186. [PubMed: 10701687]

Gilliet M, Cao W, Liu YJ. Plasmacytoid dendritic cells: sensing nucleic acids in viral infection and autoimmune diseases. Nat. Rev. Immunol. 2008; 8:594–606. [PubMed: 18641647]

Grubman MJ, Moraes MP, Diaz-San SF, Pena L, de los ST. Evading the host immune response: how foot-and-mouth disease virus has become an effective pathogen. FEMS Immunol. Med. Microbiol. 2008; 53:8–17. [PubMed: 18400012]

Harkins S, Cornell CT, Whitton JL. Analysis of translational initiation in Coxsackievirus B3 suggests an alternative explanation for the high frequency of $R_{+4}$ in the eukaryotic consensus motif. J. Virol. 2005; 79:987–996. [PubMed: 15613327]

Heath WR, Carbone FR. Dendritic cell subsets in primary and secondary T cell responses at body surfaces. Nat. Immunol. 2009; 10:1237–1244. [PubMed: 19915624]

Henke A, Huber SA, Stelzner A, Whitton JL. The role of $CD8^+$ T lymphocytes in coxsackievirus B3-induced myocarditis. J. Virol. 1995; 69:6720–6728. [PubMed: 7474082]

Hickman HD, Takeda K, Skon CN, Murray FR, Hensley SE, Loomis J, Barber GN, Bennink JR, Yewdell JW. Direct priming of antiviral $CD8^+$ T cells in the peripheral interfollicular region of lymph nodes. Nat. Immunol. 2008; 9:155–165. [PubMed: 18193049]

Huber S, Ramsingh AI. Coxsackievirus-induced pancreatitis. Viral Immunol. 2004; 17:358–369. [PubMed: 15357902]

Huhn MH, McCartney SA, Lind K, Svedin E, Colonna M, Flodstrom-Tullberg M. Melanoma differentiation-associated protein-5 (MDA-5) limits early viral replication but is not essential for the induction of type 1 interferons after Coxsackievirus infection. Virology. 2010; 401:42–48. [PubMed: 20206372]

Hunziker IP, Cornell CT, Whitton JL. Deletions within the 5'UTR of coxsackievirus B3: consequences for virus translation and replication. Virology. 2007; 360:120–128. [PubMed: 17084431]

Jakel S, Kuckelkorn U, Szalay G, Plotz M, Textoris-Taube K, Opitz E, Klingel K, Stevanovic S, Kandolf R, Kotsch K, Stangl K, Kloetzel PM, Voigt A. Differential interferon responses enhance viral epitope generation by myocardial immunoproteasomes in murine enterovirus myocarditis. Am. J. Pathol. 2009; 175:510–518. [PubMed: 19590042]

Jamieson BD, Butler LD, Ahmed R. Effective clearance of a persistent viral infection requires cooperation between virus-specific Lyt2$^{+}$ T cells and nonspecific bone marrow-derived cells. J. Virol. 1987; 61:3930–3937. [PubMed: 3500329]

Kamphuis E, Junt T, Waibler Z, Forster R, Kalinke U. Type I interferons directly regulate lymphocyte recirculation and cause transient blood lymphopenia. Blood. 2006; 108:3253–3261. [PubMed: 16868248]

Kastenmuller W, Gerner MY, Germain RN. The in situ dynamics of dendritic cell interactions. Eur. J. Immunol. 2010; 40:2103–2106. [PubMed: 20853494]

Kemball CC, Alirezaei M, Whitton JL. Type B coxsackieviruses and their interactions with the innate and adaptive immune systems. Future Microbiol. 2010a; 5:1329–1347. [PubMed: 20860480]

Kemball, CC.; Fujinami, RS.; Whitton, JL. Adaptive immune responses to picornaviruses. In: Ehrenfeld, E.; Domingo, E.; Roos, RP., editors. The Picornaviruses. Washington, DC: ASM Press; 2010b. p. 303-319.

Kemball CC, Harkins S, Whitmire JK, Flynn CT, Feuer R, Whitton JL. Coxsackievirus B3 inhibits antigen presentation in vivo, exerting a profound and selective effect on the MHC class I pathway. PLoS Path. 2009; 5:e1000618.

Kemball CC, Harkins S, Whitton JL. Enumeration and functional evaluation of virus-specific CD4$^{+}$ and CD8$^{+}$ T cells in lymphoid and peripheral sites of coxsackievirus B3 infection. J. Virol. 2008; 82:4331–4342. [PubMed: 18305030]

Knowlton KU, Jeon ES, Berkley N, Wessely R, Huber SA. A mutation in the puff region of VP2 attenuates the myocarditic phenotype of an infectious cDNA of the Woodruff variant of coxsackievirus B3. J. Virol. 1996; 70:7811–7818. [PubMed: 8892902]

Kramer M, Schulte BM, Toonen LW, de Bruijni MA, Galama JM, Adema GJ, van Kuppeveld FJ. Echovirus infection causes rapid loss-of-function and cell death in human dendritic cells. Cell. Microbiol. 2007; 9:1507–1518. [PubMed: 17298395]

Lee HK, Iwasaki A. Innate control of adaptive immunity: dendritic cells and beyond. Semin. Immunol. 2007; 19:48–55. [PubMed: 17276695]

Lee LN, Burke S, Montoya M, Borrow P. Multiple mechanisms contribute to impairment of type 1 interferon production during chronic lymphocytic choriomeningitis virus infection of mice. J. Immunol. 2009; 182:7178–7189. [PubMed: 19454715]

Leon B, Ardavin C. Monocyte-derived dendritic cells in innate and adaptive immunity. Immunol. Cell Biol. 2008; 86:320–324. [PubMed: 18362945]

Lopez-Bravo M, Ardavin C. In vivo induction of immune responses to pathogens by conventional dendritic cells. Immunity. 2008; 29:343–351. [PubMed: 18799142]

Luber CA, Cox J, Lauterbach H, Fancke B, Selbach M, Tschopp J, Akira S, Wiegand M, Hochrein H, O'Keeffe M, Mann M. Quantitative proteomics reveals subset-specific viral recognition in dendritic cells. Immunity. 2010; 32:279–289. [PubMed: 20171123]

Mena I, Fischer C, Gebhard JR, Perry CM, Harkins S, Whitton JL. Coxsackievirus infection of the pancreas: evaluation of receptor expression, pathogenesis, and immunopathology. Virology. 2000; 271:276–288. [PubMed: 10860882]

Modlin JF, Rotbart HA. Group B coxsackie disease in children. Curr. Top. Microbiol. Immunol. 1997; 223:53–80. [PubMed: 9294925]

Montoya M, Edwards MJ, Reid DM, Borrow P. Rapid activation of spleen dendritic cell subsets following lymphocytic choriomeningitis virus infection of mice: analysis of the involvement of type 1 IFN. J. Immunol. 2005; 174:1851–1861. [PubMed: 15699111]

Mukherjee A, Morosky SA, Delorme-Axford E, Dybdahl-Sissoko N, Oberste MS, Wang T, Coyne CB. The Coxsackievirus B 3C Protease Cleaves MAVS and TRIF to Attenuate Host Type I Interferon and Apoptotic Signaling. PLoS Pathog. 2011; 7:e1001311. [PubMed: 21436888]

Neznanov N, Kondratova A, Chumakov KM, Angres B, Zhumabayeva B, Agol VI, Gudkov AV. Poliovirus protein 3A inhibits tumor necrosis factor (TNF)-induced apoptosis by eliminating the TNF receptor from the cell surface. J. Virol. 2001; 75:10409–10420. [PubMed: 11581409]

Nfon CK, Toka FN, Kenney M, Pacheco JM, Golde WT. Loss of plasmacytoid dendritic cell function coincides with lymphopenia and viremia during foot-and-mouth disease virus infection. Viral Immunol. 2010; 23:29–41. [PubMed: 20121400]

Norbury CC, Malide D, Gibbs JS, Bennink JR, Yewdell JW. Visualizing priming of virus-specific $CD8^+$ T cells by infected dendritic cells in vivo. Nat. Immunol. 2002; 3:265–271. [PubMed: 11828323]

O'Connell JB. The role of myocarditis in end-stage dilated cardiomyopathy. Tex. Heart Inst. J. 1987; 14:268–275. [PubMed: 15227310]

O'Donnell DR, Carrington D. Peripheral blood lymphopenia and neutrophilia in children with severe respiratory syncytial virus disease. Pediatr. Pulmonol. 2002; 34:128–130. [PubMed: 12112779]

Okada H, Kobune F, Sato TA, Kohama T, Takeuchi Y, Abe T, Takayama N, Tsuchiya T, Tashiro M. Extensive lymphopenia due to apoptosis of uninfected lymphocytes in acute measles patients. Arch. Virol. 2000; 145:905–920. [PubMed: 10881678]

Peacock CD, Kim SK, Welsh RM. Attrition of virus-specific memory $CD8^+$ T cells during reconstitution of lymphopenic environments. J. Immunol. 2003; 171:655–663. [PubMed: 12847230]

Pircher H, Moskophidis D, Rohrer U, Burki K, Hengartner H, Zinkernagel RM. Viral escape by selection of cytotoxic T cell-resistant virus variants*in vivo* . Nature. 1990; 346:629–633. [PubMed: 1696684]

Probst HC, van den BM. Priming of CTLs by lymphocytic choriomeningitis virus depends on dendritic cells. J. Immunol. 2005; 174:3920–3924. [PubMed: 15778347]

Rahnefeld A, Ebstein F, Albrecht N, Opitz E, Kuckelkorn U, Stangl K, Rehm A, Kloetzel PM, Voigt A. Antigen-presentation capacity of dendritic cells is impaired in ongoing enterovirus myocarditis. Eur. J. Immunol. 2011

Rhoades RE, Tabor-Godwin JM, Tsueng G, Feuer R. Enterovirus infections of the central nervous system. Virology. 2011; 411:288–305. [PubMed: 21251690]

Romero JR. Pediatric group B coxsackievirus infections. Curr. Top. Microbiol. Immunol. 2008; 323:223–239. [PubMed: 18357772]

Schattner A, Meshorer A, Wallach D. Involvement of interferon in virus-induced lymphopenia. Cell Immunol. 1983; 79:11–25. [PubMed: 6861209]

Schulte BM, Kramer M, Ansems M, Lanke KH, van Doremalen N, Piganelli JD, Bottino R, Trucco M, Galama JM, Adema GJ, van Kuppeveld FJ. Phagocytosis of enterovirus-infected pancreatic β-cells triggers innate immune responses in human dendritic cells. Diabetes. 2010; 59:1182–1191. [PubMed: 20071599]

Segura E, Villadangos JA. Antigen presentation by dendritic cells in vivo. Curr. Opin. Immunol. 2009; 21:105–110. [PubMed: 19342210]

Shen Z, Reznikoff G, Dranoff G, Rock KL. Cloned dendritic cells can present exogenous antigens on both MHC class I and class II molecules. J. Immunol. 1997; 158:2723–2730. [PubMed: 9058806]

Shortman K, Heath WR. The $CD8^+$ dendritic cell subset. Immunol. Rev. 2010; 234:18–31. [PubMed: 20193009]

Slifka MK, Pagarigan RR, Mena I, Feuer R, Whitton JL. Using recombinant coxsackievirus B3 to evaluate the induction and protective efficacy of $CD8^+$ T cells during picornavirus infection. J. Virol. 2001; 75:2377–2387. [PubMed: 11160741]

Slifka MK, Whitton JL. Functional avidity maturation of $CD8^+$ T cells without selection of higher affinity TCR. Nat. Immunol. 2001; 2:711–717. [PubMed: 11477407]

Sole MJ, Liu P. Viral myocarditis: a paradigm for understanding the pathogenesis and treatment of dilated cardiomyopathy. J. Am. Coll. Cardiol. 1993; 22:99A–105A. [PubMed: 8509572]

Swiecki M, Colonna M. Accumulation of plasmacytoid DC: Roles in disease pathogenesis and targets for immunotherapy. Eur. J. Immunol. 2010a; 40:2094–2098. [PubMed: 20853492]

Swiecki M, Colonna M. Unraveling the functions of plasmacytoid dendritic cells during viral infections, autoimmunity, and tolerance. Immunol. Rev. 2010b; 234:142–162. [PubMed: 20193017]

Tabor-Godwin JM, Ruller CM, Bagalso N, An N, Pagarigan RR, Harkins S, Gilbert PE, Kiosses WB, Gude NA, Cornell CT, Doran KS, Sussman MA, Whitton JL, Feuer R. A novel population of myeloid cells responding to coxsackievirus infection assists in the dissemination of virus within the neonatal CNS. J. Neurosci. 2010; 30:8676–8691. [PubMed: 20573913]

Tam PE. Coxsackievirus myocarditis: Interplay between virus and host in the pathogenesis of heart disease. Viral Immunol. 2006; 19:133–146. [PubMed: 16817756]

Tracy, S.; Chapman, NM. Group B coxsackievirus diseases. In: Ehrenfeld, E.; Domingo, E.; Roos, RP., editors. Picornaviruses: Molecular Biology, Evolution and Pathogenesis. ASM; 2010. p. 353-368.

van Houten N, Bouchard PE, Moraska A, Huber SA. Selection of an attenuated Coxsackievirus B3 variant, using a monoclonal antibody reactive to myocyte antigen. J. Virol. 1991; 65:1286–1290. [PubMed: 1847455]

Varela-Calvino R, Skowera A, Arif S, Peakman M. Identification of a naturally processed cytotoxic CD8 T-cell epitope of coxsackievirus B4, presented by HLA-A2.1 and located in the PEVKEK region of the P2C nonstructural protein. J. Virol. 2004; 78:13399–13408. [PubMed: 15564450]

Villadangos JA, Schnorrer P. Intrinsic and cooperative antigen-presenting functions of dendritic-cell subsets in vivo. Nat. Rev. Immunol. 2007; 7:543–555. [PubMed: 17589544]

Villadangos JA, Young L. Antigen-presentation properties of plasmacytoid dendritic cells. Immunity. 2008; 29:352–361. [PubMed: 18799143]

Voigt A, Jakel S, Textoris-Taube K, Keller C, Drung I, Szalay G, Klingel K, Henklein P, Stangl K, Kloetzel PM, Kuckelkorn U. Generation of in silico predicted coxsackievirus B3-derived MHC class I epitopes by proteasomes. Amino Acids. 2010; 39:243–255. [PubMed: 19997756]

Wahid R, Cannon MJ, Chow M. Dendritic cells and macrophages are productively infected by poliovirus. J. Virol. 2005; 79:401–409. [PubMed: 15596833]

Wang JP, Asher DR, Chan M, Kurt-Jones EA, Finberg RW. Cutting Edge: Antibody-mediated TLR7-dependent recognition of viral RNA. J. Immunol. 2007; 178:3363–3367. [PubMed: 17339429]

Wang JP, Cerny A, Asher DR, Kurt-Jones EA, Bronson RT, Finberg RW. MDA5 and MAVS mediate type I IFN responses to Coxsackie B virus. J. Virol. 2010; 84:254–260. [PubMed: 19846534]

Weinzierl AO, Rudolf D, Maurer D, Wernet D, Rammensee HG, Stevanovic S, Klingel K. Identification of HLA-A*01- and HLA-A*02-restricted $CD8^+$ T-cell epitopes shared among group B enteroviruses. J. Gen. Virol. 2008a; 89:2090–2097. [PubMed: 18753217]

Weinzierl AO, Szalay G, Wolburg H, Sauter M, Rammensee HG, Kandolf R, Stevanovic S, Klingel K. Effective chemokine secretion by dendritic cells and expansion of cross-presenting $CD4^-/CD8^+$ dendritic cells define a protective phenotype in the mouse model of coxsackievirus myocarditis. J. Virol. 2008b; 82:8149–8160. [PubMed: 18550677]

Weslow-Schmidt JL, Jewell NA, Mertz SE, Simas JP, Durbin JE, Flano E. Type I interferon inhibition and dendritic cell activation during gammaherpesvirus respiratory infection. J. Virol. 2007; 81:9778–9789. [PubMed: 17626106]

Wessely R, Klingel K, Knowlton KU, Kandolf R. Cardioselective infection with coxsackievirus B3 requires intact type I interferon signaling: implications for mortality and early viral replication. Circulation. 2001; 103:756–761. [PubMed: 11156890]

Whitmire JK, Benning N, Whitton JL. Precursor frequency, nonlinear proliferation, and functional maturation of virus-specific $CD4^+$ T cells. J. Immunol. 2006; 176:3028–3036. [PubMed: 16493061]

Whitmire JK, Eam B, Whitton JL. Tentative T cells : memory cells are quick to respond, but slow to divide. PLoS Path. 2008; 4:1–11.

Whitton JL. Immunopathology during coxsackievirus infection. Springer Semin. Immunopathol. 2002; 24:201–213. [PubMed: 12503065]

Wilson NS, Behrens GM, Lundie RJ, Smith CM, Waithman J, Young L, Forehan SP, Mount A, Steptoe RJ, Shortman KD, de Koning-Ward TF, Belz GT, Carbone FR, Crabb BS, Heath WR, Villadangos JA. Systemic activation of dendritic cells by Toll-like receptor ligands or malaria

infection impairs cross-presentation and antiviral immunity. Nat. Immunol. 2006; 7:165–172. [PubMed: 16415871]

Young LJ, Wilson NS, Schnorrer P, Mount A, Lundie RJ, La Gruta NL, Crabb BS, Belz GT, Heath WR, Villadangos JA. Dendritic cell preactivation impairs MHC class II presentation of vaccines and endogenous viral antigens. Proc. Natl. Acad. Sci. U. S. A. 2007; 104:17753–17758. [PubMed: 17978177]

Young LJ, Wilson NS, Schnorrer P, Proietto A, ten BT, Matsuki Y, Mount AM, Belz GT, O'Keeffe M, Ohmura-Hoshino M, Ishido S, Stoorvogel W, Heath WR, Shortman K, Villadangos JA. Differential MHC class II synthesis and ubiquitination confers distinct antigen-presenting properties on conventional and plasmacytoid dendritic cells. Nat. Immunol. 2008; 9:1244–1252. [PubMed: 18849989]

Zuniga EI, Liou LY, Mack L, Mendoza M, Oldstone MB. Persistent virus infection inhibits type I interferon production by plasmacytoid dendritic cells to facilitate opportunistic infections. Cell Host Microbe. 2008; 4:374–386. [PubMed: 18854241]

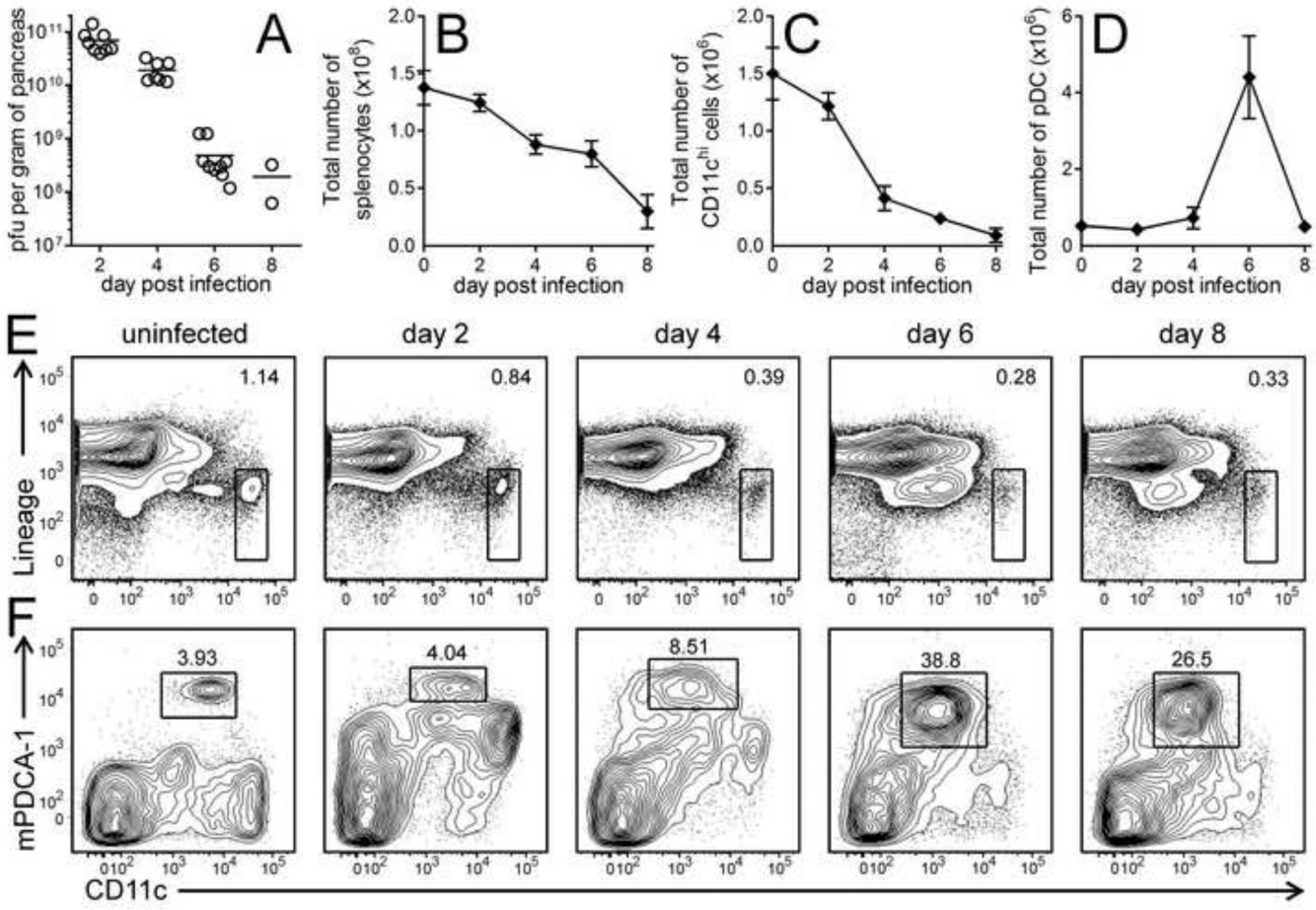


**Figure 1. CVB3 infection substantially alters the numbers of conventional and plasmacytoid dendritic cells in vivo**

Mice were infected with wtCVB3, and the virus titers in the pancreas (A, titers shown for individual mice, with mean) and total number of mononuclear cells in the spleen (B) were determined at the indicated time points p.i. Data show the mean ± SEM of 2–12 mice per time point, combined from 4 independent experiments. Conventional and plasmacytoid DCs in the spleen were analyzed by flow cytometry on days 2, 4, 6, and 8 p.i. (C) Total number of cDCs in the spleen. (D) Total number of pDCs in the spleen. Data show the mean ± SEM of 2–9 mice per time point, combined from 3 independent experiments. Representative contour plots are shown, and the rectangular gates identify cDCs [$CD11c^{hi}$ and lineage negative ($CD3^{-}CD19^{-}CD49b^{-}$), panel E] and pDCs [$CD11c^{int}$ and mPDCA-$1^{hi}$ (plots are gated on lineage negative cells), panel F]; the numbers shown on the contour plots are the percentages of conventional or plasmacytoid DCs among all cells in the plot.

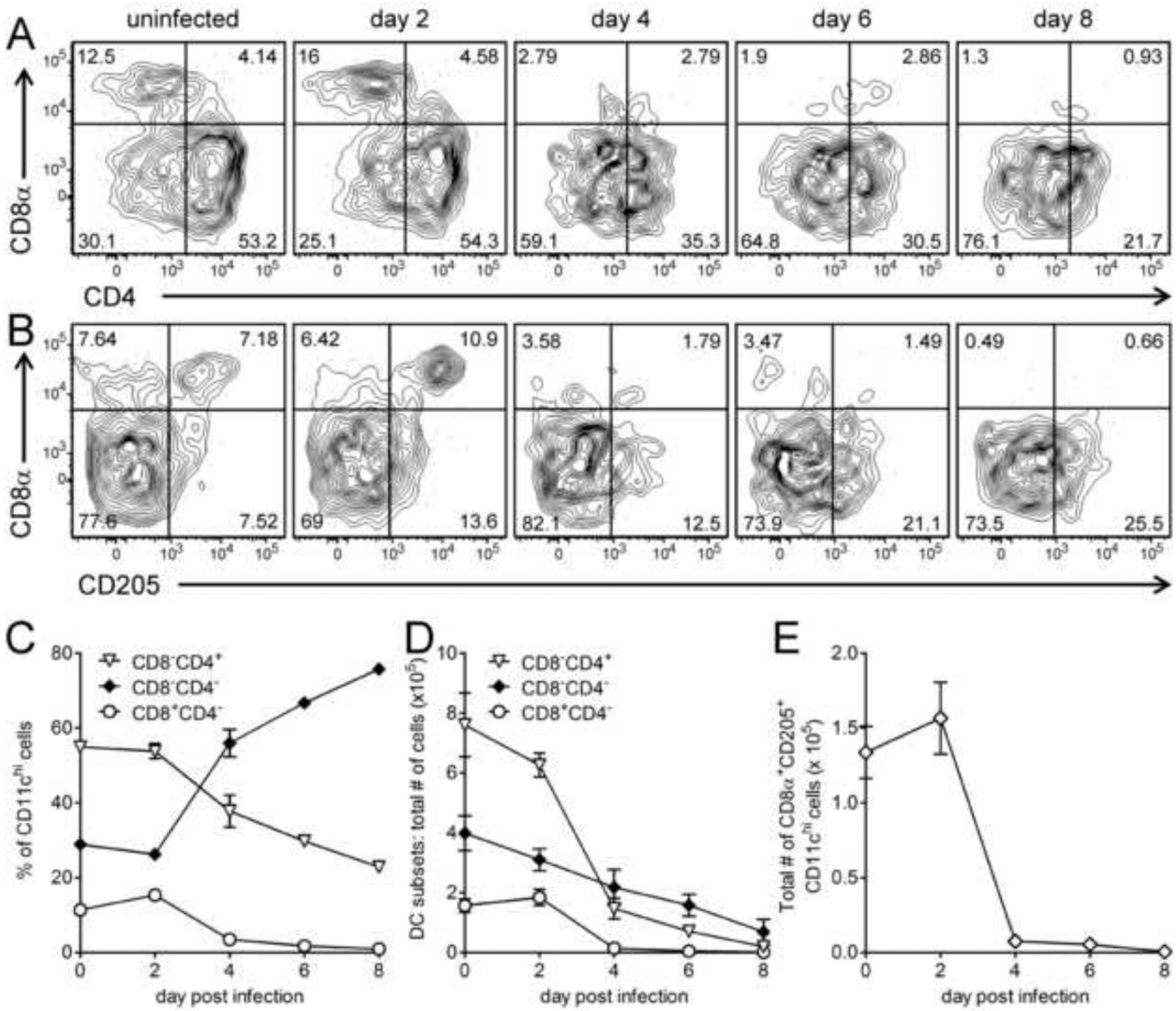


**Figure 2. CVB3 infection profoundly reduces the numbers of CD8α$^+$, CD4$^+$, and double negative conventional dendritic cells**

Mice were infected with wtCVB3, and splenocytes were harvested and analyzed by flow cytometry on days 2, 4, 6, and 8 p.i. Representative contour plots are shown (A & B), and were gated to include CD11c$^{hi}$ lineage$^{neg}$ cells. The numbers indicate the proportion of the various subsets of cDCs (CD8α$^+$, CD4$^+$, double negative, and CD8α$^+$CD205$^+$) in each quadrant, as a percentage of all CD11c$^{hi}$ lineage$^{neg}$ cells. (C) Frequency of CD8α$^+$, CD4$^+$, and double negative cDCs (as a percentage of CD11c$^{hi}$ lineage$^{neg}$ cells) in the spleen. (D) Total number of CD8α$^+$, CD4$^+$, double negative cDCs in the spleen. (E) Total number of CD8α$^+$CD205$^+$ cDCs in the spleen. Data show the mean ± SEM of 2–9 mice per time point, combined from 3 independent experiments.

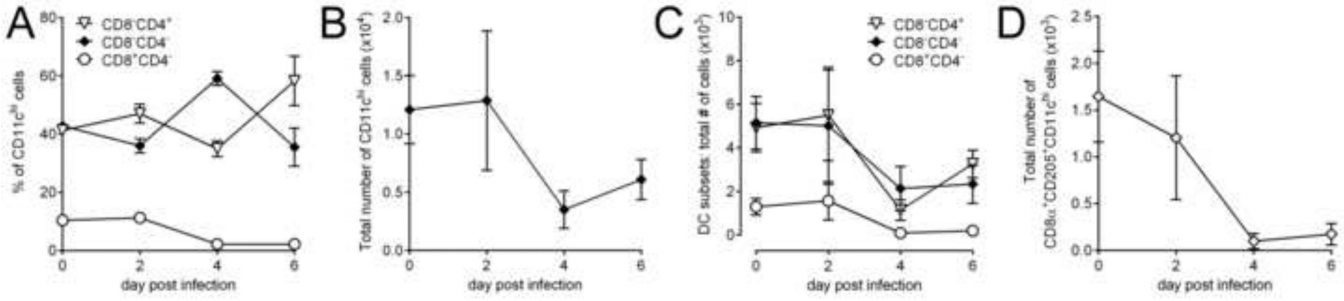


**Figure 3. CVB3 infection diminishes the number of conventional dendritic cells in lymph nodes**

Mice were infected with wtCVB3, and lymphocytes were harvested from pancreatic lymph nodes (pLNs) and analyzed by flow cytometry on days 2, 4, and 6 p.i. (A) Frequency of $CD8\alpha^+$, $CD4^+$, and double negative cDCs (as a percentage of $CD11c^{hi}$ $lineage^{neg}$ cells) in the pLNs. (B) Total number of $CD11c^{hi}$ cDCs in the pLNs. (C) Total number of $CD8\alpha^+$, $CD4^+$, and double negative cDCs in the pLNs. (D) Total number of $CD8\alpha^+CD205^+$cDCs in the pLNs. Data show the mean ± SEM of 3–4 mice per time point, combined from 2 independent experiments.

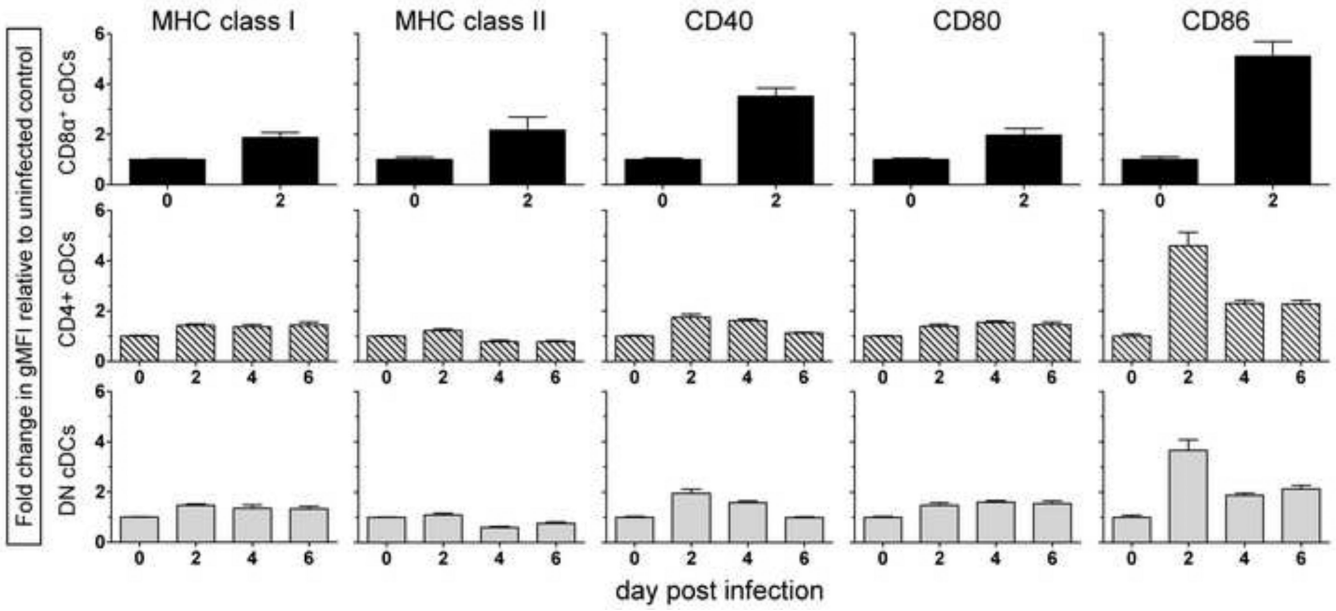


**Figure 4. Conventional dendritic cells up-regulate the expression of MHC and costimulatory molecules following virus infection**

Mice were infected with wtCVB3, and the level of cell surface expression of MHC class I, MHC class II, CD40, CD80, and CD86 on cDCs in the spleen was measured by flow cytometry on day 2, 4, and 6. The expression kinetics for MHC and costimulatory molecules are shown for each of the 3 major cDC subsets ($CD8\alpha^+$, top row; $CD4^+$, middle row; and double negative, bottom row). The fold change in the geometric mean fluorescence intensity of each protein over the course of infection was normalized and compared to the level of expression on cells from uninfected mice (day 0). Data show the mean + SEM of 4–9 mice per time point, combined from 3 independent experiments. The expression level of these proteins on the $CD8\alpha^+$ subset could not be determined after day 2 because these cells were too few in number.

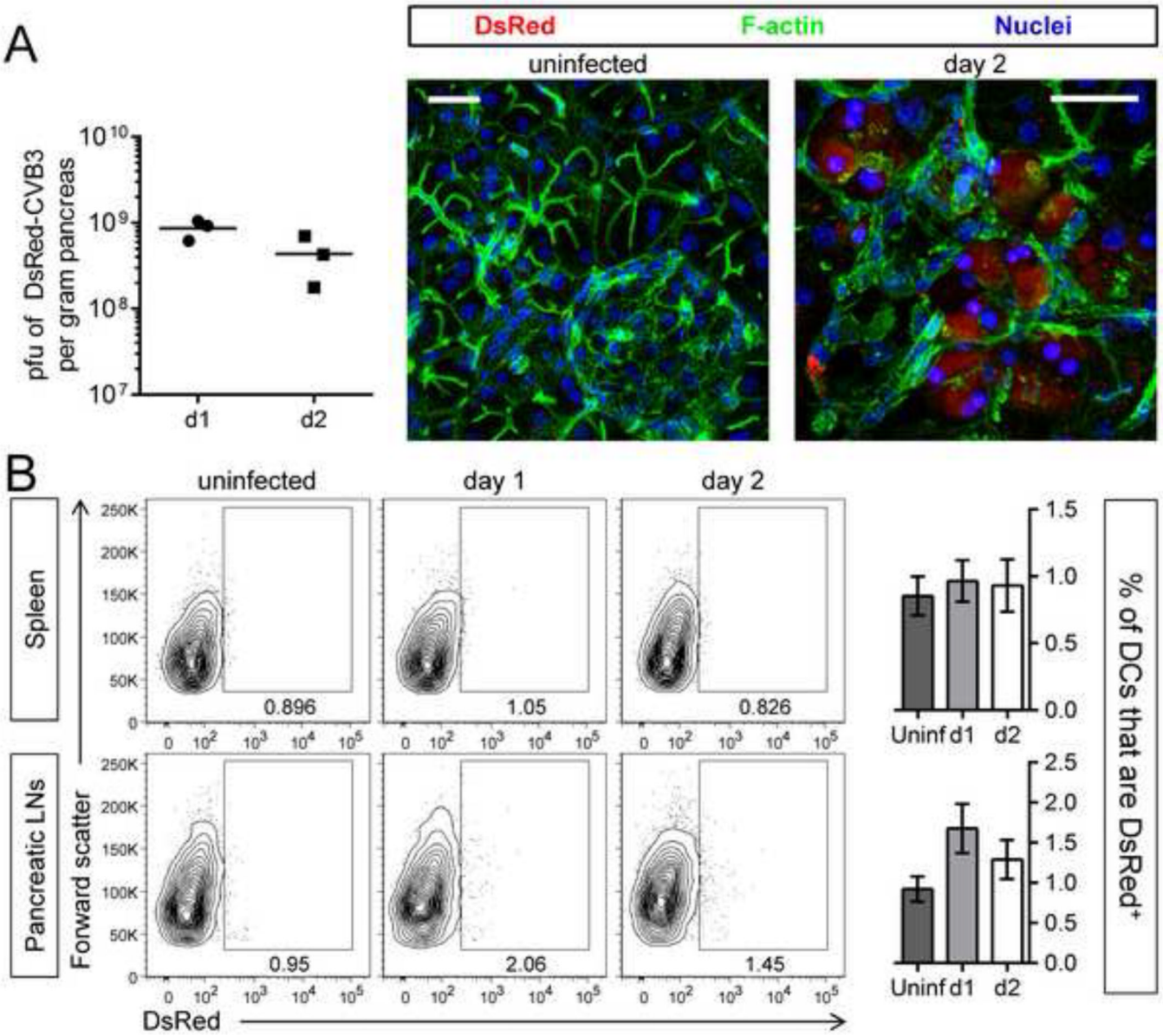


**Figure 5. Few, if any, dendritic cells are infected by CVB3 in vivo**

Mice were infected with DsRed-CVB3, and were sacrificed 1 or 2 days later. (A) Viral titers in the pancreas were measured (graph) and DsRed protein was imaged by confocal microscopy of vibratome sections of pancreas; scale bar = 30 μm. (B) The frequency of $DsRed^+$ DCs in the spleen and pancreatic lymph nodes was analyzed by flow cytometry on days 1 and 2. Contour plots are gated on DCs [$CD11c^{hi}$ and "lineage" negative ($CD3^-CD19^-$ $CD49b^-$) cells for the spleen (top row), and $CD11c^{int\text{-}hi}$ $lineage^-$ cells for the pancreatic lymph nodes (bottom row)]. The large rectangular gates shown on representative contour plots identify $DsRed^+$ cells, and the numbers shown are the percentage of $DsRed^+$ cells among all cells in the plot. ~3–7.5×$10^3$ DCs were analyzed in these plots. Bar graphs display the mean ± SEM of 3 mice per group. No statistically significant differences were detected among these groups by a t-test.

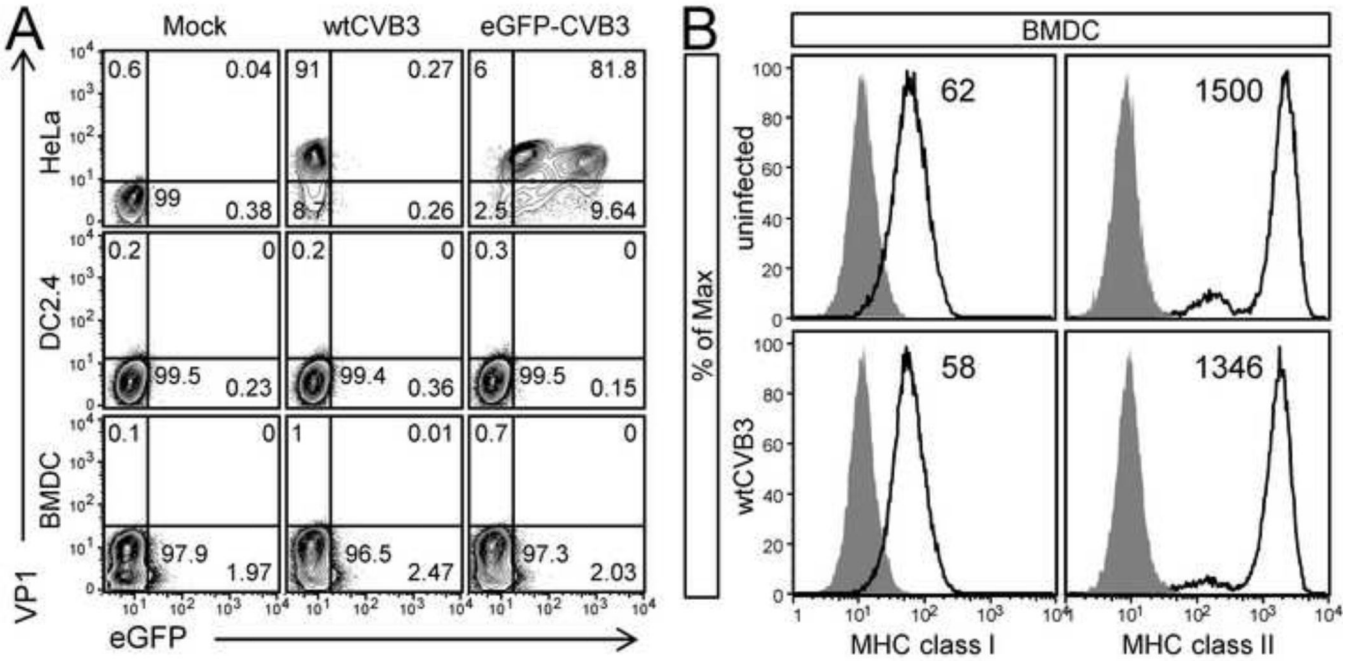


**Figure 6. wtCVB3 has little effect on dendritic cells in vitro**

(A) Bone marrow monocyte-derived dendritic cells (BMDCs) and the DC2.4 dendritic cell line were evaluated for their susceptibility to CVB3 infection; HeLa cells were infected as a positive control. HeLa, DC2.4, and BMDCs were incubated with wtCVB3 or eGFP-CVB3 (MOI=10) for 1 hr, or mock infected. Inoculum was removed, and cells were harvested (HeLa cells, 6 hrs p.i.; BMDC & DC2.4, 24 hrs p.i.), stained for intracellular VP1, and the percentage of cells expressing VP1 ± eGFP was determined by flow cytometry. Representative contour plots are shown for each cell type, and the numbers indicate the proportion of cells in each quadrant, as a percentage of all cells in the plot ($VP1^+$, upper left quadrant; $eGFP^+$, lower right quadrant; $VP1^+eGFP^+$, upper right quadrant). (B) BMDCs (cultured with GM-CSF) were infected with wtCVB3 (MOI=100), or left uninfected, and the surface expression of MHC class I and II were analyzed by flow cytometry 18 hrs p.i. Histograms are gated on $CD11c^+CD11b^+$ cells, and show the expression of MHC class I or II (black lines); isotype control staining is shaded grey. The number on each histogram indicates the geometric mean fluorescence intensity of MHC class I or II. Data are representative of 2 independent experiments.

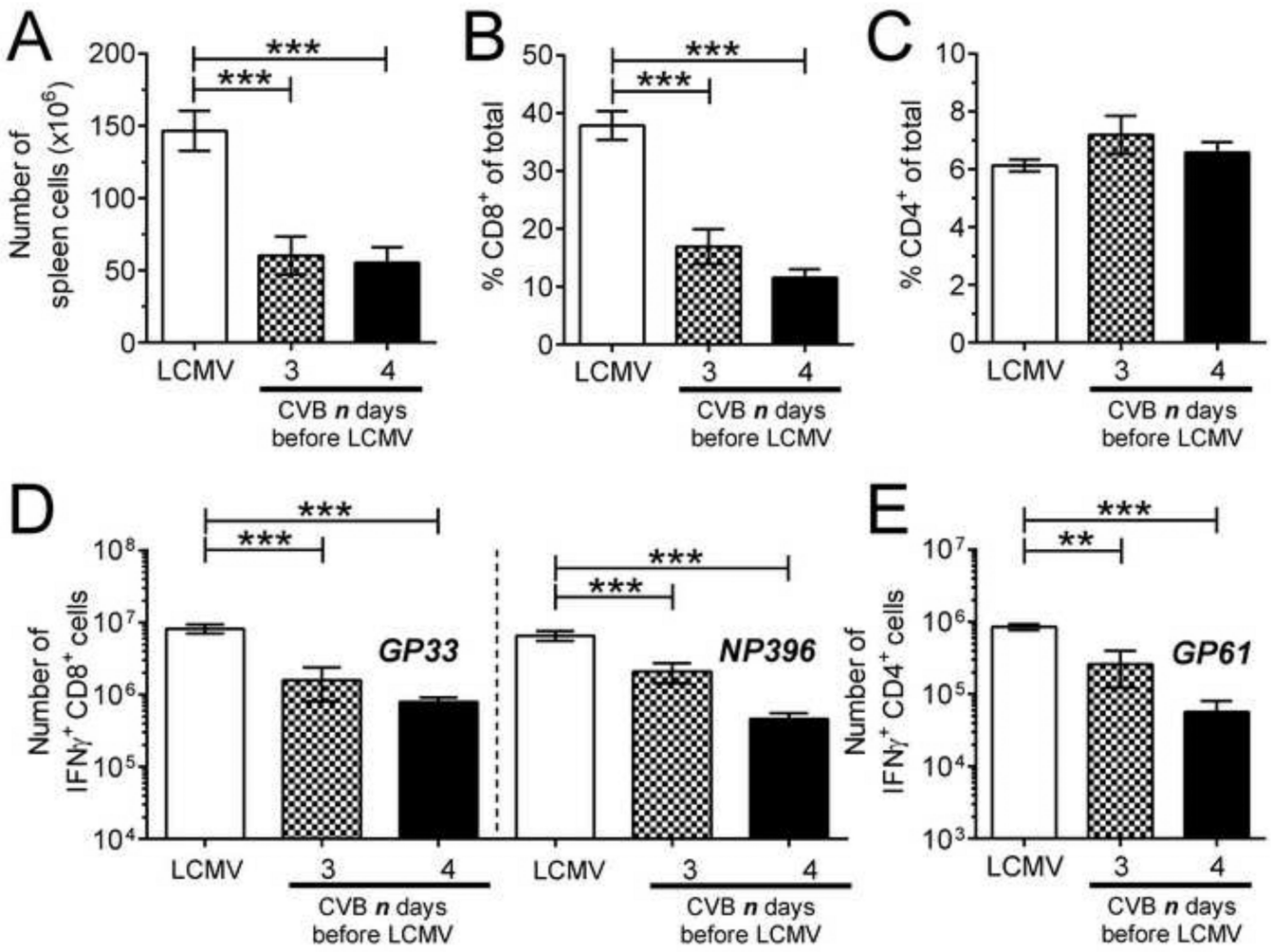


**Figure 7. CVB3-infected mice mount weaker CD4$^+$ and CD8$^+$ T cell responses to a secondary virus infection**

Groups of mice were infected with wtCVB3, and then co-infected with LCMV (3 or 4 days after the primary infection with CVB3). An additional group of mice was infected only with LCMV. LCMV-specific CD8$^+$ and CD4$^+$ T cell responses were analyzed 7 days after LCMV infection by flow cytometry. (A) Total number of mononuclear cells in the spleen. (B & C) Frequency of CD8$^+$ and CD4$^+$ T cells in the spleen, as a percentage of total mononuclear cells. (D & E) Splenocytes were stimulated with peptide, and the total numbers of T cells producing IFNγ in response to $GP_{33}$ & $NP_{396}$ peptides (D), and $GP_{61}$ peptide (E) were determined by flow cytometry. Data show the mean ± SEM of 6 or 8 mice per group, combined from 2 independent experiments (** $p<0.01$, *** $p<0.001$).

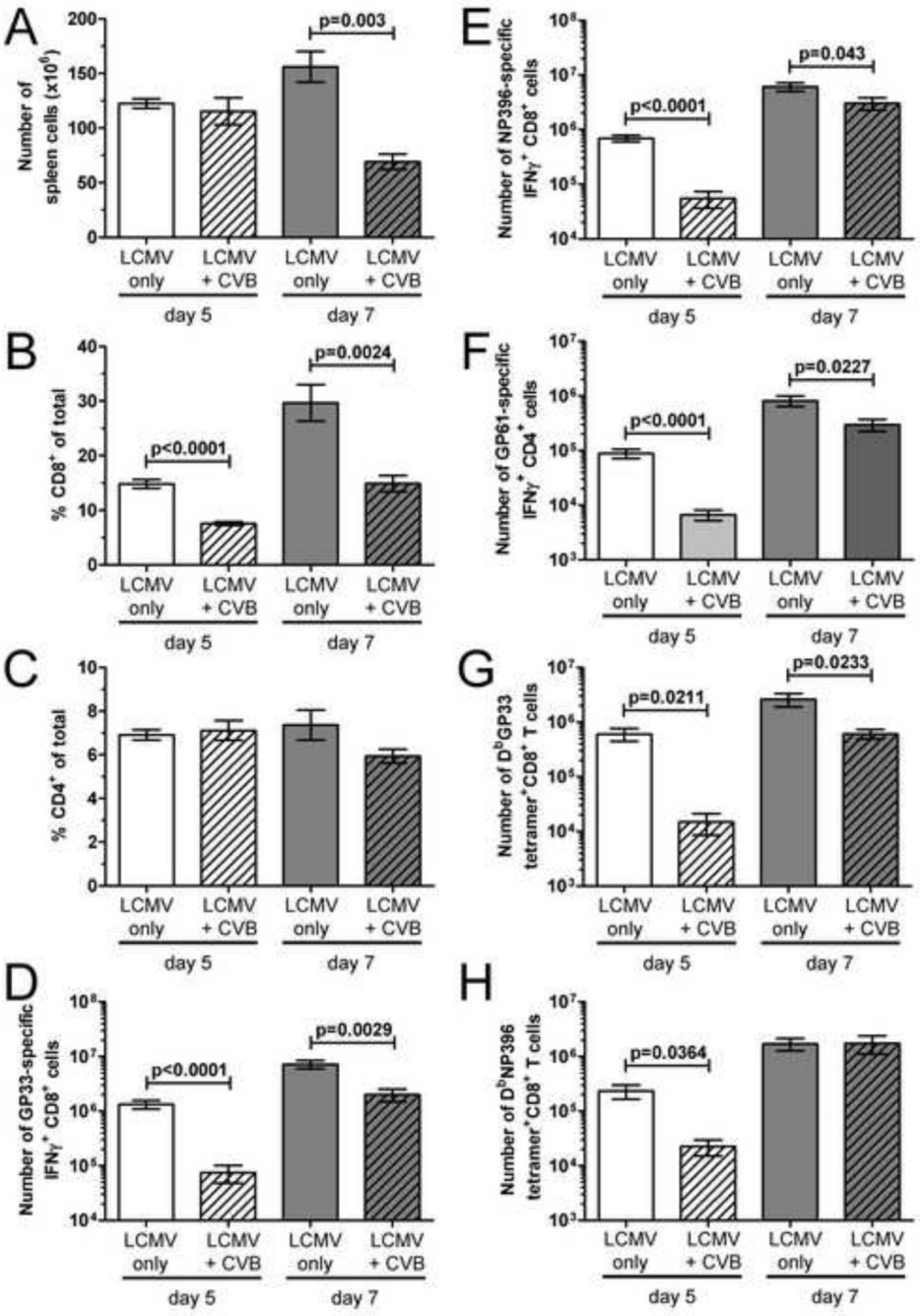


**Figure 8. The effect of wtCVB3 infection is more profound at the early stage of LCMV-specific T cell expansion**

Mice were infected with wtCVB3 and co-infected with LCMV 2 days later. An additional group of mice was infected only with LCMV. LCMV-specific $CD8^+$ and $CD4^+$ T cell responses were analyzed 5 or 7 days after LCMV infection by flow cytometry. (A) Total number of mononuclear cells in the spleen. (B & C) Frequency of $CD8^+$ and $CD4^+$ T cells in the spleen, as a percentage of total mononuclear cells. (D, E, & F) Splenocytes were stimulated with peptide, and the total numbers of T cells producing IFNγ in response to $GP_{33}$ (D), $NP_{396}$ (E), and $GP_{61}$ peptides (F) were determined by flow cytometry. Data show the mean ± SEM of 6 or 8 mice per group, combined from 3 independent experiments. (G &

H) The total number of $D^bGP_{33}$ and $D^bNP_{396}$ tetramer$^+$ CD8$^+$ T cells in the spleen was determined by flow cytometry. Data show the mean ± SEM of 3 or 4 mice per group, combined from 2 independent experiments. Statistical significance was determined by an unpaired t-test.

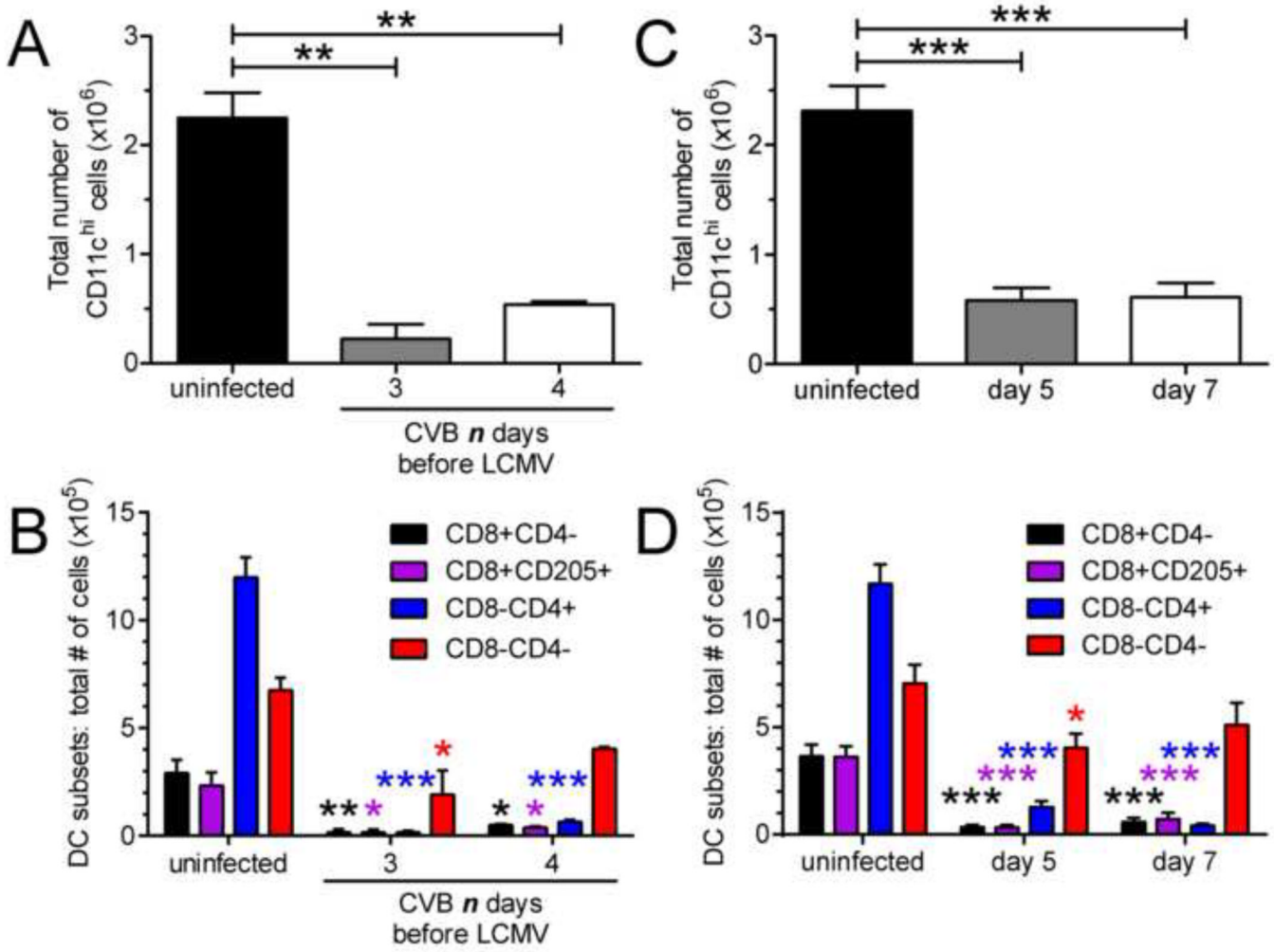


**Figure 9. Conventional dendritic cell numbers are diminished in co-infected mice**

Groups of mice were infected with wtCVB3, and then co-infected with LCMV. (A & B) Mice received LCMV 3 or 4 days after the primary infection with CVB3, and cDCs were analyzed 7 days after LCMV infection by flow cytometry. (C & D) Mice received LCMV 2 days after CVB3, and cDCs were analyzed on day 5 and 7 after LCMV infection. (A & C) Total number of cDCs in the spleen. (B & D) Total number of $CD8\alpha^+$, $CD8\alpha^+CD205^+$, $CD4^+$, and double negative cDCs in the spleen. Data show the mean ± SEM of 2 or 3 mice per group (A & B), or 6–8 mice per group combined from 3 independent experiments (C & D). Statistically significant differences between uninfected and co-infected groups were detected by ANOVA (* $p<0.05$, ** $p<0.01$, *** $p<0.001$).

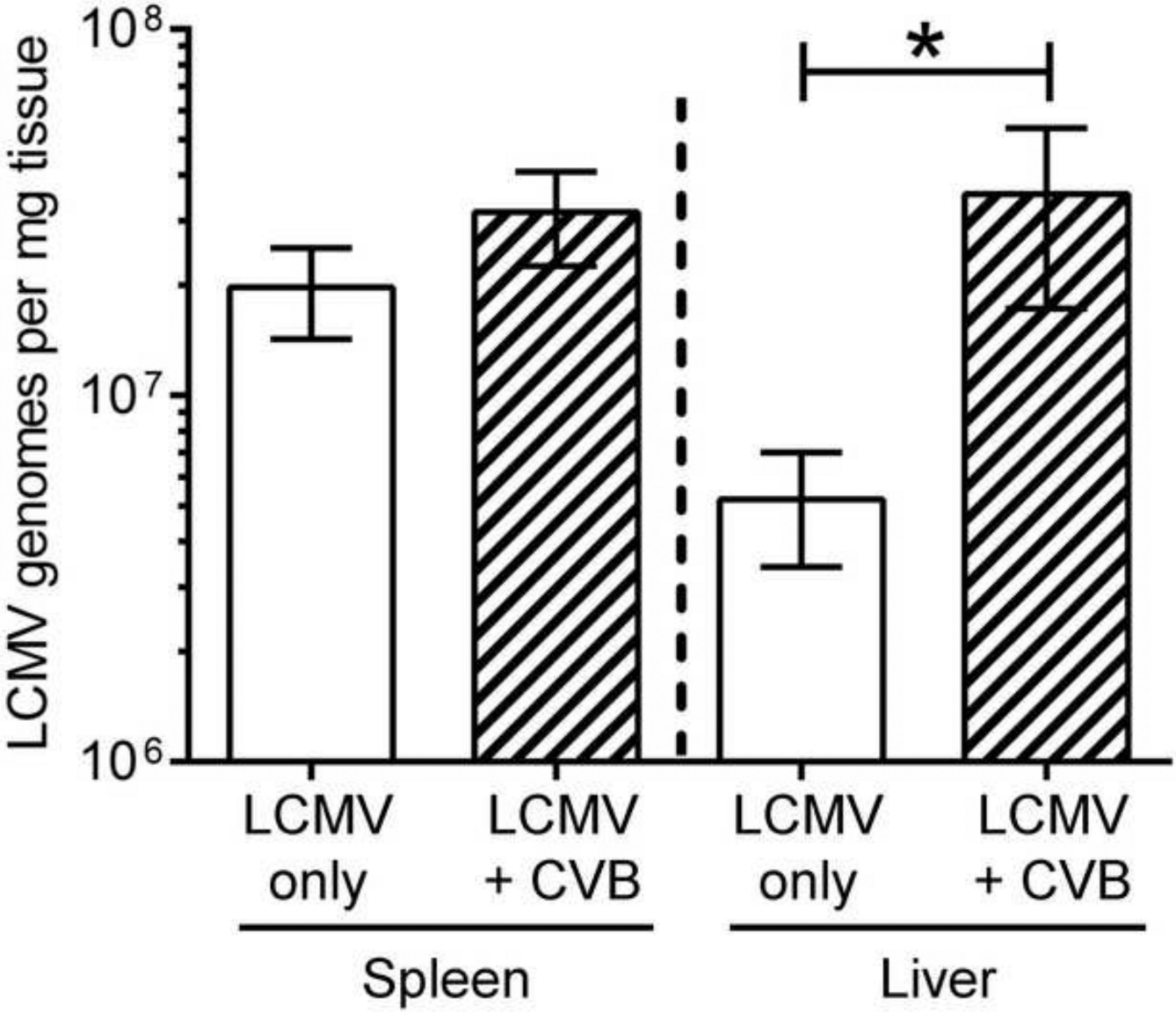


**Figure 10. CVB3 infection does not dampen LCMV replication in co-infected mice**

Mice were infected with wtCVB3 and then co-infected with LCMV 2 days later. Another group of mice received only LCMV. Five days after LCMV infection, RNA was isolated from the spleen and liver and the number of LCMV genomes was determined by quantitative real time RT-PCR. Data show the mean ± SEM of 3 or 6 mice per group, combined from 2 independent experiments (* $p<0.05$, determined by an unpaired t-test).

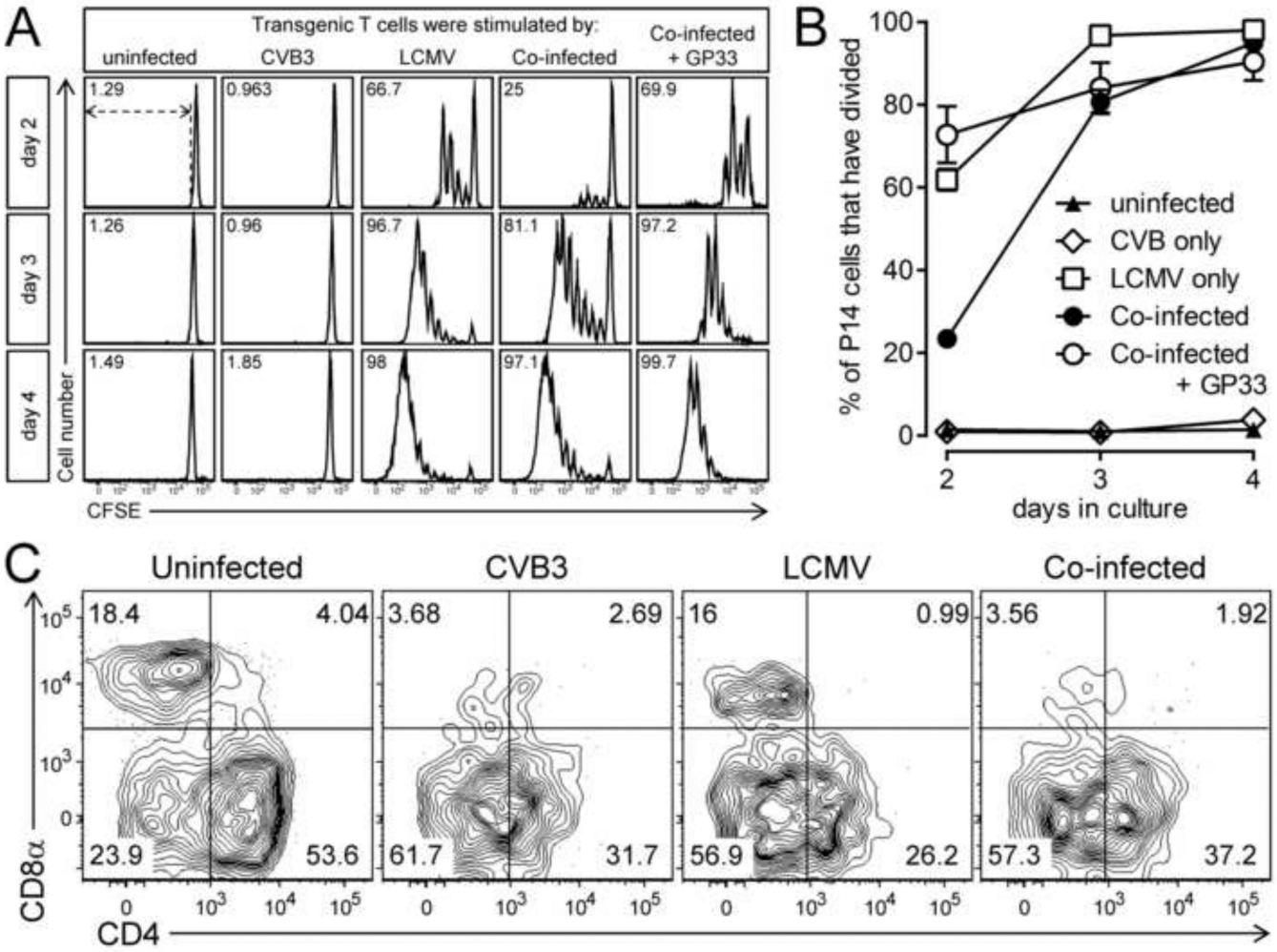


**Figure 11. In vitro stimulation assay: wtCVB3 delays, but does not prevent, expansion of LCMV-specific CD8+ T cells**

Mice were infected with wtCVB3 and, 4 days later, were co-infected with LCMV. Control mice received CVB3 alone, LCMV alone, or no virus. Splenocytes were harvested from infected mice 2 days after LCMV infection and/or 6 days post CVB3, and were incubated *in vitro* with magnetically purified, CFSE-labeled, P14 $CD8^+$ transgenic T cells. An additional set of cultures included P14 cells incubated with splenocytes from co-infected mice + 1 μM $GP_{33–41}$ peptide. Duplicate wells were harvested on days 2, 3, or 4, and analyzed by flow cytometry. (A) Proliferation (loss of CFSE fluorescence) of P14 T cells. Histograms are gated on $CD8^+Thy1.1^+$ cells, and, for each histogram, the percentage of P14 cells that have divided is shown; the gate used to define P14 division is shown by dotted lines in the upper left panel. (B) Kinetics of P14 T cell division *in vitro*. Data show the percentage of total P14 cells in each well that have divided at least once, and are expressed as the mean ± SEM of 3–7 mice per group (n=1 for P14 cells incubated with uninfected control splenocytes). (C) The frequency of cDC subsets in the splenocyte stimulator populations (prior to *in vitro* culture) was determined by flow cytometry. Representative contour plots are shown, and are gated on $CD11c^{hi}$ $lineage^{neg}$ cells. The numbers indicate the proportion of cells in each quadrant, as a percentage of all $CD11c^{hi}$ $lineage^{neg}$ cells.

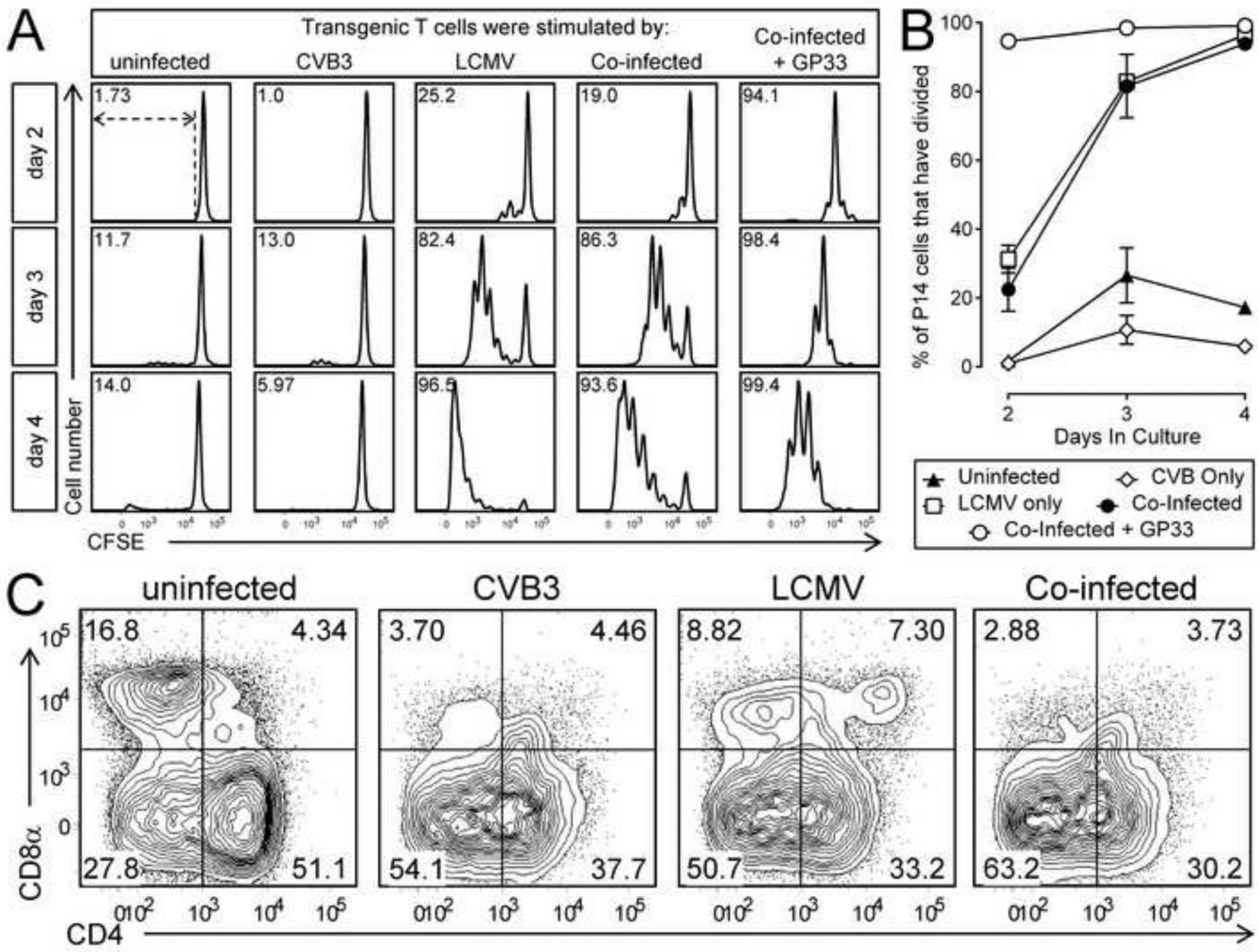


**Figure 12. Purified dendritic cells from LCMV-infected or co-infected mice are similarly capable of stimulating T cell proliferation in vitro**

Mice were infected with wtCVB3 and, 4 days later, were co-infected with LCMV. Control mice received CVB3 alone, LCMV alone, or no virus. Splenocytes were harvested from infected mice 2 days after LCMV infection and/or 6 days post CVB3, and $CD11c^{hi}$ DCs were purified by magnetic enrichment (splenocytes were pooled within mouse groups). Naïve $CD8^+$ transgenic T cells were also purified by magnetic enrichment from uninfected P14 mice, and then labeled with CFSE. An equal number ($6\times10^4$/well) of purified DCs from each group were incubated with purified P14 T cells ($1.2\times10^5$/well) *in vitro*. An additional set of cultures included P14 cells incubated with $GP_{33–41}$ peptide-pulsed purified DCs from co-infected mice. Culture wells were harvested on days 2, 3, or 4, and analyzed by flow cytometry. (A) Proliferation (loss of CFSE fluorescence) of P14 T cells. Histograms are gated on $CD8^+Thy1.1^+$ cells, and, for each histogram, the percentage of P14 cells that have divided is shown; the gate used to define P14 division is shown by dotted lines in the upper left panel. (B) Kinetics of P14 T cell division *in vitro*. Data show the percentage of total P14 cells in each well that have divided at least once, and are expressed as the mean ± SEM of triplicate wells. (C) Prior to the start of *in vitro* culture, the purified DC stimulator populations were analyzed by flow cytometry to determine the frequency of cDCs subsets. Representative contour plots are gated on $CD11c^{hi}$ $lineage^{neg}$ cells. The numbers indicate

the proportion of the cDC subset ($CD8\alpha^+$, $CD4^+$, double negative) in each quadrant, as a percentage of all $CD11c^{hi}$ $lineage^{neg}$ cells.